Parametric modeling for damped sinusoids from multiple channels

Zhou, Zhenhua; So, Hing Cheung; Christensen, Mads Græsbøll

Published in:
I E E E Transactions on Signal Processing

DOI (link to publication from Publisher):
10.1109/TSP.2013.2260334

Publication date:
2013

Document Version
Publisher's PDF, also known as Version of record

Parametric Modeling for Damped Sinusoids From Multiple Channels

Zhenhua Zhou, H. C. So, *Senior Member, IEEE*, and Mads Græsbøll Christensen, *Senior Member, IEEE*

***Abstract*—The problem of parametric modeling for noisy damped sinusoidal signals from multiple channels is addressed. Utilizing the shift invariance property of the signal subspace, the number of distinct sinusoidal poles in the multiple channels is first determined. With the estimated number, the distinct frequencies and damping factors are then computed with the multi-channel weighted linear prediction method. The estimated sinusoidal poles are then matched to each channel according to the extreme value theory of distribution of random fields. Simulations are performed to show the performance advantages of the proposed multi-channel sinusoidal modeling methodology compared with existing methods.**

***Index Terms*—Extreme value theory, model order estimation, multi-channel processing, sinusoidal model selection, sinusoidal parameter estimation, weighted linear prediction.**

I. Introduction

PARAMETRIC modeling for sinusoidal signals [1] is a classical but still open problem in statistical signal processing, finding its applications in a wide range of areas. This problem consists of two parts — sinusoidal model order detection and parameter estimation. During the recent decades, the problem of parametrically modeling the sinusoidal signals from multiple channels, which are contaminated by different undesired harmonics [2]–[8], has attracted considerable attention. For example, in the fields of nuclear magnetic resonance and nuclear quadrupole resonance spectroscopy, the measured signals in different channels are well modeled as a sum of exponentially damped sinusoids [9], and may share common mode sinusoidal components. In music and voiced speech signal processing, the signals recorded using a microphone array can be modeled as a sum of harmonic signals with different sinusoidal orders, fundamental frequencies and directions-of-arrival (DOAs) [6]. Given the corresponding observations, the goal is to determine the unknown orders and the parameters of the sinusoids in the multiple channels, after which the signal parametrization is complete. This problem is of great research value not just because it is interesting and practical, but also there are two significant advantages compared to single-channel modeling:

- The multi-channel setup means more observed data and the parameter estimation refinement of the common mode sinusoidal components is expected, which makes it feasible to extract the common information in a more accurate way. This is evident from the Cramér-Rao lower bound (CRLB) [10] and comparison with single-channel results, as shown in Section V.
- In a multi-source scenario, if the sources are overlapping in one dimension (e.g., for a multi-pitch signal [11], the sources share some harmonic components), a single-channel setup will not be able to resolve the sources. On the other hand, this issue can be solved with the multi-channel setup (e.g., for the multi-pitch signal, we can observe the sources using a microphone array, and model them with joint DOA and fundamental frequency estimation [6]–[8]).

The main contribution of this work is on parametric modeling of multi-channel sinusoidal signals. Here, we focus on the general case of damped cisoids. Recently, there have been several proposals to achieve multi-channel damped sinusoidal parameter estimation. In [12], two decimative versions of the Hankel total least-squares (HTLS) approach, that is, HTLSDstack and HTLSDsum algorithms, are proposed, where the decimative data can be regarded as a special case of multi-channel signals with the same sinusoidal components. Similar ideas have also been applied to the spectral analysis of multi-channel magnetic resonance spectroscopy data [3]. To deal with a more general multi-channel sinusoidal parameter estimation problem where the signals in different channels consist of different sinusoidal components, the signal subspaces of all the single channels are computed with the singular value decomposition (SVD), the common signal subspace is extracted with a second SVD, and the common poles, where each corresponds to a pair of frequency and damping factor, are found from the common signal subspace using total least squares (TLS) [2], [4]. There also exist other methods to tackle the multi-channel estimation problem, such as principal component analysis (PCA) [13] and independent component analysis (ICA) [14]. However, these algorithms cannot perform optimally with respect to the CRLB as they are not derived from maximum likelihood (ML) framework. What is more important is that all of the above methods do not take the problem of model order detection into account, namely, the detection of the numbers of the sinusoidal components existing in the channels and especially the number of the common sinusoidal poles, which are assumed known $a\ priori$. Additionally, the remaining sinusoidal components, which do not appear in all the channels, reflect the character-

Manuscript received August 17, 2012; revised January 27, 2013 and April 18, 2013; accepted April 19, 2013. Date of publication April 26, 2013; date of current version July 10, 2013. The associate editor coordinating the review of this manuscript and approving it for publication was Prof. Antonio Napolitano.

Z. Zhou and H. C. So are with the Department of Electronic Engineering, City University of Hong Kong, Hong Kong, China (e-mail: sjtu.zzh2010@gmail.com; hcso@ee.cityu.edu.hk).

M. G. Christensen is with Audio Analysis Lab, Department of Architecture, Design and Media Technology, Aalborg University, Aalborg 9220, Denmark (e-mail: mgc@create.aau.dk).

Color versions of one or more of the figures in this paper are available online at http://ieeexplore.ieee.org.

Digital Object Identifier 10.1109/TSP.2013.2260334

istics of their corresponding channels [4], [5], and are also of interest. But the aforementioned [2]–[4], [12]–[14] do not pay attention to them.

In this paper, we aim at addressing these issues from a new and complete viewpoint via performing the parametric modeling with joint model selection and parameter estimation. It consists of three parts: (i) detection of the number of distinct sinusoidal poles from multiple channels; (ii) optimal frequency and damping factor estimation of the distinct sinusoidal poles; and (iii) sinusoidal model selection, that is, matching the estimated sinusoidal poles to their corresponding channels.

In the literature [15], there are many methods to detect the number of sinusoids embedded in noise. For the undamped sinusoids, detection schemes include the information theoretic criteria [16], [17] such as the minimum description length (MDL) criterion, direct Kullback-Leibler (KL) approach, generalized cross-validatory KL approach based on the generalized information criterion (GIC), Bayesian approach based on the Bayesian information criterion (BIC). However, all of them are based on the asymptotic conditions of infinite data lengths. Therefore, they cannot be applied to the damped sinusoidal signal indeed, which decays to zero with sufficiently large data length. Recently, several methods have been proposed [18]–[20] for the tone number detection of damped sinusoids, which are related to the rank determination of data matrix. In [18], the MUltiple SIgnal Classification (MUSIC) order estimator is devised by means of the subspace angles. But performance loss will occur when the frequency spacing is not large, especially for damped sinusoids, which is seen from the derivation of the order estimation measure. Both ESTimation ERror (ESTER) [19] and subspace-based automatic model order selection (SAMOS) [20] methods are developed to determine the rank of data matrix and to detect the tone number with the use of the shift-invariance property of signal subspace. The latter is more robust to noise because it takes into account the perturbation of both sides of the shift-invariance equation instead of computing the residual error of the shift-invariance equation in a least squares (LS) sense. Here we extend the SAMOS method to the multi-channel scenario, and detect the number of the distinct sinusoidal poles in the multiple channels with the multi-channel model order estimator (MC-MOE).

From the detected number of the distinct multi-channel sinusoidal poles, the next step is to estimate the corresponding frequencies and damping factors. It is well known that the ML method [21] is statistically efficient while its computational complexity is extremely high, especially when the tone number is large, which limits its use in practice. Instead, computationally efficient techniques have been proposed, such as the subspace-based algorithms [22], [23], linear prediction-based methods [24], [25], and weighted linear prediction (WLP) [26] estimators. In particular, the WLP-based estimators are popular with good computational efficiency and nearly optimum estimation accuracy. Usually they consider the single-channel signal. Here, we extend the WLP approach to the current problem, that is, parameter estimation for the sinusoidal poles from multiple channels, which is referred to as the multi-channel weighted linear prediction (MC-WLP) estimator.

Finally, sinusoidal model selection, or matching the estimated poles to their corresponding channels, is realized based on a sequence of hypothesis tests. At each test, we compute the significance of the maximum correlation between the estimation residual and a sinusoidal function, whose statistical property is derived from the extreme value theory (EVT) about the distribution of the maximum of stochastic fields. We refer this scheme to as EVT selector.

The rest of this paper is organized as follows. The problem of parametric modeling for damped sinusoids from multiple channels is formulated in Section II. The proposed methodology for model selection and sinusoidal parameter estimation is presented in Section III, which includes detecting the number of the distinct sinusoidal poles with the MC-MOE, sinusoidal parameter estimation with the MC-WLP method, and sinusoidal model selection for each channel with the EVT selector. Monte Carlo simulation results are presented in Section V to evaluate the performance of the proposed framework by comparing with other popular order detection and multi-channel sinusoidal parameter estimation methods. Finally, conclusions are drawn in Section VI.

II. Problem Formulation

The observed data are noisy multi-channel damped cisoids without reverberation and multi-path components [2]–[4], and they are modeled as:

$$x_k(n) = s_k(n) + v_k(n) = \sum_{m=1}^{M_k} \rho_{k,m} z_{k,m}^n + v_k(n), \qquad (1)$$

where $z_{k,m} = e^{-\alpha_{k,m}+j\omega_{k,m}}$, $n = 1, 2, \ldots, N$, $k = 1, 2, \ldots, K$, and $m = 1, 2, \ldots, M_k$, with $\rho_{k,m}, \omega_{k,m} \in [0, 2\pi)$ and $\alpha_{k,m} \geq 0$ being the unknown complex-valued amplitude, frequency and damping factor of the m-th sinusoidal component in the k-th channel, respectively. The $K \geq 2$ and M_k represent the number of channels and sinusoidal components in the k-th channel, respectively, while $N \gg \max\{M_1, M_2, \ldots, M_K\}$ represents the data length. Here, M_k, $k = 1, 2, \ldots, K$, are assumed not all to be zero, and $v_k(n)$ is the additive noise source in the k-th channel, $k = 1, 2, \ldots, K$, which is assumed to be uncorrelated white complex Gaussian process with mean zero and variance σ_k^2. According to [2]–[5], [27], the sinusoidal poles $z_{k,m}$, $m = 1, 2, \ldots, M_k$, from different channels indexed $k = 1, 2, \ldots, K$, may be shared by K or less channels, which means that $z_{k,m}$ from the channels $\mathbf{\Omega} \subseteq \{1, 2, \ldots, K\}$ are identical. Such sinusoidal poles correspond to the common mode information.

Our objective is to estimate the frequencies and damping factors of the sinusoidal components in the multiple channels, and to determine the sinusoidal model of each channel by matching the estimated sinusoidal poles to their corresponding channels. Since the common mode information is shared by multiple channels, better estimation accuracy is expected.

III. Algorithm Development

A. Detection of Distinct Multi-Channel Sinusoidal Poles

In [20], the SAMOS method is proposed for order detection of single-channel damped sinusoids, which consists of constructing the data matrix, analyzing the shift-invariance of the signal subspace, and determining the rank information of data

matrix. Here, we develop the MC-MOE for detection of the number of the distinct sinusoidal poles in the multiple channels by extending the SAMOS method, where we will construct the multi-channel data matrix and analyze its rank information.

For the k-th channel, $k = 1, 2, \ldots, K$, define an $L \times (N - L + 1)$ Hankel matrix as:

$$\overline{\mathbf{X}}_k = \mathbf{S}_k + \mathbf{Q}_k, \tag{2}$$

where $\overline{\mathbf{X}}_k$ is the $L \times (N - L + 1)$ data matrix with the (l, n)-th element $[\overline{\mathbf{X}}_k]_{l,n} = x_k(l + n - 1)$, and the row number L satisfying $2 \cdot \max\{M_1, M_2, \ldots, M_K\} + 1 < L < N + 1$. The matrices $\mathbf{S}_k$ and $\mathbf{Q}_k$ are the noise-free and noise components of $\overline{\mathbf{X}}_k$, respectively. From (1), the Vandermonde decomposition of the Hankel matrix $\mathbf{S}_k$ can be written as:

$$\mathbf{S}_k = \mathbf{A}_k \mathbf{\Xi}_k \mathbf{H}_k^T, \tag{3}$$

$$\mathbf{A}_k = [\mathbf{a}_{k,1}\ \mathbf{a}_{k,2}\ \ldots\ \mathbf{a}_{k,M_k}],$$

$$\mathbf{a}_{k,l} = \left[z_{k,l}\ z_{k,l}^2\ \cdots\ z_{k,l}^L\right]^T, \tag{4}$$

$$\mathbf{H}_k = [\mathbf{h}_{k,1}\ \mathbf{h}_{k,2}\ \ldots\ \mathbf{h}_{k,M_k}],$$

$$\mathbf{h}_{k,l} = \left[1\ z_{k,l}\ \cdots\ z_{k,l}^{N-L}\right]^T, \tag{5}$$

$$\mathbf{\Xi}_k = \mathrm{diag}(\rho_{k,1},\ \rho_{k,2},\ \ldots,\ \rho_{k,M_k}), \tag{6}$$

for $l = 1, 2, \ldots, M_k$. In the following, we explore the rank property of the signal subspace of the multi-channel signal and extend the SAMOS method to estimate the number of the distinct sinusoidal poles in the multiple channels, denoted by M.

Firstly, we group and re-index the distinct sinusoidal poles $z_{k,m} = e^{-\alpha_{k,m} + j\omega_{k,m}}$, $m = 1, 2, \ldots, M_k$, from the K channels, $k = 1, 2, \ldots, K$, as $z_m = e^{-\alpha_m + j\omega_m}$, $m = 1, 2, \ldots, M$. Stack the data matrices $\overline{\mathbf{X}}_k$, $k = 1, 2, \ldots, K$, as $\overline{\mathbf{X}} = [\,\overline{\mathbf{X}}_1\ \ \overline{\mathbf{X}}_2\ \ \ldots\ \ \overline{\mathbf{X}}_K\,]$, which can be expressed as:

$$\overline{\mathbf{X}} = \mathbf{S} + \mathbf{Q}, \tag{7}$$

with $\mathbf{S}$ and $\mathbf{Q}$ being the noise-free and noise components, respectively. According to (3), $\mathbf{S}$ can be decomposed as:

$$\begin{aligned}\mathbf{S} &= [\,\mathbf{S}_1\ \ \mathbf{S}_2\ \ \ldots\ \ \mathbf{S}_K\,] \\ &= \mathbf{A}\,[\,\mathbf{\Gamma}_1\mathbf{H}^T\ \ \mathbf{\Gamma}_2\mathbf{H}^T\ \ \ldots\ \ \mathbf{\Gamma}_K\mathbf{H}^T\,],\end{aligned} \tag{8}$$

where

$$\mathbf{A} = [\mathbf{a}_1\ \mathbf{a}_2\ \cdots\ \mathbf{a}_M],\ \mathbf{a}_l = \left[z_l\ z_l^2\ \ldots\ z_l^L\right]^T, \tag{9}$$

$$\mathbf{H} = [\mathbf{h}_1\ \mathbf{h}_2\ \ldots\ \mathbf{h}_M],\ \mathbf{h}_l = \left[1\ z_l\ \ldots\ z_l^{N-L}\right]^T, \tag{10}$$

$$\mathbf{\Gamma}_k = \mathrm{diag}(\varrho_{k1}, \varrho_{k2}, \ldots, \varrho_{kM}), \tag{11}$$

for $l = 1, 2, \ldots, M$, and

$$\varrho_{kl} = \begin{cases} \rho_{k,i}, & \text{if } \exists\, i, 1 \le i \le M_k, \text{: } e^{-\alpha_{k,i} + j\omega_{k,i}} = e^{-\alpha_l + j\omega_l}; \\ 0, & \text{otherwise.} \end{cases} \tag{12}$$

From (8), it is observed that $\mathbf{S}$ is rank-M and its column space is exactly spanned by the M Vandermonde columns of $\mathbf{A}$ with the following shift-invariance property:

$$\mathbf{A}_\uparrow = \mathbf{A}_\downarrow \mathbf{D}, \tag{13}$$

where $\mathbf{D} = \mathrm{diag}(z_1, z_2, \ldots, z_M)$ and the subscripts $\uparrow$ and $\downarrow$ denote the first and last row-deleting operators, respectively. On the other hand, due to the rank-M property, $\mathbf{S}$ can be decomposed using the SVD as:

$$\mathbf{S} = \mathbf{U}\mathbf{\Lambda}\mathbf{V}^H = [\mathbf{U}_s\ \mathbf{U}_n] \begin{bmatrix} \mathbf{\Lambda}_s & \mathbf{0} \\ \mathbf{0} & \mathbf{0} \end{bmatrix} [\mathbf{V}_s\ \mathbf{V}_n]^H, \tag{14}$$

where $\mathbf{U}_s \in \mathbb{C}^{L \times M}$ and $\mathbf{V}_s \in \mathbb{C}^{(N-L+1)K \times M}$, and $\mathbf{U}_n \in \mathbb{C}^{L \times (L-M)}$ and $\mathbf{V}_n \in \mathbb{C}^{(N-L+1)K \times (N-L+1)K-M}$ are the components of signal and noise subspaces, respectively, and $\mathbf{\Lambda}_s \in \mathbb{C}^{M \times M}$ is a diagonal matrix with non-zero diagonal elements. Comparing (14) and (8), it is seen that the columns of $\mathbf{U}_s$ span the same space as that of $\mathbf{A}$. Therefore, $\mathbf{U}_s$ is also rank-M, and bears the shift-invariance property:

$$\mathbf{U}_{s\uparrow} = \mathbf{U}_{s\downarrow} \mathbf{\Phi}, \tag{15}$$

where $\mathbf{\Phi} = \mathbf{Q}_0 \mathbf{D} \mathbf{Q}_0^{-1}$ with $\mathbf{Q}_0$ being a unitary matrix. From (15), we see that $\mathbf{U}_{s\uparrow}$ and $\mathbf{U}_{s\downarrow}$ span exactly the same subspace, and then $\mathbf{U}_s^{tb} = [\,\mathbf{U}_{s\uparrow}\ \ \mathbf{U}_{s\downarrow}\,] \in \mathbb{C}^{(L-1) \times 2M}$ is still a rank-M matrix. This means that the last M singular values of $\mathbf{U}_s^{tb}$ are equal to zero. According to the principle of the SAMOS method [28], the number of the distinct poles in the K channels is estimated as:

$$\hat{M} = \arg\min_{\tilde{M}} E(\tilde{M}), \tag{16}$$

for $1 \le \tilde{M} < \min\{(L-1)/2, L - M + 1\}$, with

$$E(\tilde{M}) = \frac{1}{\tilde{M}} \sum_{i=\tilde{M}+1}^{2\tilde{M}} \hat{\gamma}_i, \tag{17}$$

where $\hat{\gamma}_i$ is the i-th largest singular value of $\hat{\mathbf{U}}_s^{tb} \in \mathbb{C}^{(L-1) \times 2\tilde{M}}$, which is constructed from the left $\tilde{M}$ columns of the left singular matrix of $\overline{\mathbf{X}}$. This method is referred to as MC-MOE.

B. Frequency and Damping Factor Estimation

Having determined M, we estimate the sinusoidal poles z_m, $m = 1, 2, \ldots, M$, to obtain the frequency and damping factor parameters. In the past years, several sinusoidal parameter estimation methods [22]–[25] with low computational complexity but suboptimal performance have been developed. To improve the estimation accuracy, our development is based on the WLP technique [29]. Since the WLP-based method originates from the optimum weighting of error, nearly optimum estimation accuracy is expected.

To begin with, it is observed that there exists a coefficient vector $\mathbf{a} = [a_1\ a_2\ \ldots\ a_M]^T$ such that $f_1(z) = z^M + \sum_{m=1}^M a_m z^{M-m}$ and $f_2(z) = \prod_{m=1}^M (z - z_m)$ are equivalent, and then $f_1(z_m) = f_2(z_m) = 0$, for $m = 1, 2, \ldots, M$. Thus,

$$s_k(n) + \sum_{m=1}^{M} a_m s_k(n-m) = \sum_{i=1}^{M_k} z_{k,i}^{n-M} \cdot f_1(z_{k,i}) = 0, \tag{18}$$

for $n = M + 1, M + 2, \ldots, N$, $k = 1, 2, \ldots, K$, that is, the noise-free signal $s_k(n)$ satisfies the linear prediction (LP) relation of (18). Here, the elements in $\mathbf{a}$ are the LP coefficients.

When the signal is corrupted by noise, (18) will not be satisfied exactly. Instead, the LP error vector for the k-th channel, $k = 1, 2, \ldots, K$, is:

$$\mathbf{e}_k = \mathbf{X}_k \tilde{\mathbf{a}} - \mathbf{b}_k, \tag{19}$$

where

$$\begin{aligned} \mathbf{X}_k = &\text{Toeplitz}\big([x_k(M) \;\; x_k(M+1) \;\; \ldots \;\; x_k(N-1)]^T, \\ &[x_k(M) \;\; x_k(M-1) \;\; \ldots \;\; x_k(1)] \big), \end{aligned} \tag{20}$$

$$\mathbf{b}_k = -[\, x_k(M+1) \quad x_k(M+2) \quad \ldots \quad x_k(N)\,]^T. \tag{21}$$

Here $\text{Toeplitz}(\mathbf{p}_1, \mathbf{p}_2^T)$ denotes the Toeplitz matrix with $\mathbf{p}_1$ and $\mathbf{p}_2^T$ as the first column and first row, respectively, and $\tilde{\mathbf{a}}$ is the variable for $\mathbf{a}$. Stack the K LP error vectors $\mathbf{e}_k$, $k = 1, 2, \ldots, K$, as $\mathbf{e} = [\mathbf{e}_1^T \;\; \mathbf{e}_2^T \;\; \ldots \;\; \mathbf{e}_K^T]^T$. According to WLP, the LP coefficient estimates, denoted by $\hat{\mathbf{a}}$, are determined by solving the following cost function:

$$\begin{aligned} \hat{\mathbf{a}} &= \arg\min_{\tilde{\mathbf{a}}} \mathbf{e}^H \mathbf{W} \mathbf{e} \\ &= \arg\min_{\tilde{\mathbf{a}}} (\mathbf{X}\tilde{\mathbf{a}} - \mathbf{b})^H \mathbf{W} (\mathbf{X}\tilde{\mathbf{a}} - \mathbf{b}), \end{aligned} \tag{22}$$

where $\mathbf{X} = [\mathbf{X}_1^T \;\; \mathbf{X}_2^T \;\; \ldots \;\; \mathbf{X}_K^T]^T$, $\mathbf{b} = [\mathbf{b}_1^T \;\; \mathbf{b}_2^T \;\; \ldots \;\; \mathbf{b}_K^T]^T$ are formed by stacking $\mathbf{X}_k$, $\mathbf{b}_k$, $k = 1, 2, \ldots, K$, and $\mathbf{W}$ is the weighting matrix, which has the form of [30]:

$$\begin{aligned} \mathbf{W} &= \left[E\left\{ \mathbf{e}\mathbf{e}^H \right\} \right]^{-1} \\ &= \text{blkdiag}\left(\sigma_1^{-2}\mathbf{W}_0 \;\; \sigma_2^{-2}\mathbf{W}_0 \;\; \ldots \;\; \sigma_K^{-2}\mathbf{W}_0 \right), \end{aligned} \tag{23}$$

where $\mathbf{W}_0 = \left(\mathbf{A}_0 \mathbf{A}_0^H \right)^{-1}$, and $\mathbf{A}_0 = \text{Hankel}\big([\mathbf{0}_{1\times(N-M-1)}, 1]^T, [1 \;\; \tilde{a}_1 \;\; \ldots \;\; \tilde{a}_M \;\; \mathbf{0}_{1\times(N-M-1)}] \big)$ with $\text{Hankel}(\mathbf{p}_1, \mathbf{p}_2^T)$ denoting the Hankel matrix with $\mathbf{p}_1$ and $\mathbf{p}_2^T$ as the first column and last row, respectively. Relaxing the weighting matrix $\mathbf{W}$ as known *a priori*, the WLP solution to (22) is:

$$\hat{\mathbf{a}} = \left(\sum_{k=1}^{K} \sigma_k^{-2} \mathbf{X}_k^H \mathbf{W}_0 \mathbf{X}_k \right)^{-1} \left(\sum_{k=1}^{K} \sigma_k^{-2} \mathbf{X}_k^H \mathbf{W}_0 \mathbf{b}_k \right). \tag{24}$$

The estimates of the sinusoidal poles existing in the multiple channels, $\hat{z}_1, \hat{z}_2, \ldots, \hat{z}_M$, can be obtained as the M roots of the following LP equation:

$$z^M + \sum_{m=1}^{M} \hat{a}_m z^{M-m} = 0, \tag{25}$$

and the corresponding estimates of the frequency and damping factor of the m-th sinusoidal pole $\hat{z}_m$, denoted by $\hat{\omega}_m$, $\hat{\alpha}_m$, are

$$\hat{\omega}_m = \angle \hat{z}_m, \quad \hat{\alpha}_m = -\ln(|\hat{z}_m|). \tag{26}$$

In practice, $\mathbf{a}$ and $\left\{ \sigma_k^2 \right\}_{k=1}^K$, which are required in constructing the weighting matrix $\mathbf{W}$ of (23), are not known *a priori*. Accordingly, $\hat{\mathbf{a}}$ and $\{\hat{\alpha}_m\}_{m=1}^M$, $\{\hat{\omega}_m\}_{m=1}^M$ are computed in an iterative manner:

- Step 1. Set the noise levels as $\hat{\sigma}_k^2 = 1$, $k = 1, 2, \ldots, K$.
- Step 2. Determine the initial estimate $\hat{\mathbf{a}}$ from (24) by setting $\mathbf{W}_0$ as $\mathbf{I}_N$, which denotes the $N \times N$ identity matrix.
- Step 3. Use $\hat{\mathbf{a}}$ and $\left\{ \hat{\sigma}_k^2 \right\}_{k=1}^K$ to construct the weighting matrix $\mathbf{W}$, and find an updated estimate $\hat{\mathbf{a}}$.
- Step 4. Estimate the sinusoidal poles $\{\hat{z}_m\}_{m=1}^M$ from $\hat{\mathbf{a}}$ by solving the roots of (25).
- Step 5. Use $\{\hat{z}_m\}_{m=1}^M$ to estimate the noise levels as

$$\hat{\sigma}_k^2 = \mathbf{x}_k^H (\mathbf{I}_N - \hat{\mathbf{\Theta}}(\hat{\mathbf{\Theta}}^H \hat{\mathbf{\Theta}})^{-1} \hat{\mathbf{\Theta}}^H) \mathbf{x}_k / N,$$

  for $k = 1, 2, \ldots, K$, where

$$\begin{aligned} \hat{\mathbf{\Theta}} &= \left[\hat{\boldsymbol{\theta}}_1 \quad \hat{\boldsymbol{\theta}}_2 \quad \ldots \quad \hat{\boldsymbol{\theta}}_M \right], \\ \hat{\boldsymbol{\theta}}_m &= \left[\hat{z}_m, \, \hat{z}_m^2, \, \ldots, \, \hat{z}_m^N \right]^T, \\ \mathbf{x}_k &= \left[x_k(1), \, x_k(2), \, \ldots, \, x_k(N) \right]^T. \end{aligned}$$

- Step 6. Repeat Step 3 — Step 5 until the difference of the 2-norm of $\hat{\mathbf{a}}$ between successive iterations is smaller than 10^{-13}, and then the final estimates $\hat{\mathbf{a}}$ and $\{\hat{z}_m\}_{m=1}^M$ are obtained.

This method is called the multi-channel weighted linear prediction (MC-WLP) estimator.

It is worth mentioning that when the unknown noise levels $\sigma_1^2, \sigma_2^2, \ldots, \sigma_K^2$, are equal, they will be canceled in the first and second terms of (24). As a result, the procedure to estimate the noise levels in Step 5 can be eliminated.

C. Sinusoidal Model Selection for Multiple Channels

Up to now, we have estimated the number of the distinct poles in the multiple channels and the corresponding frequencies and damping factors. However, it is still unknown which sinusoidal poles belong to which channel. This is a problem of sinusoidal model selection, namely, matching the estimated sinusoidal poles to their corresponding channels. For convenience of analysis, we assume that M_k are all nonzero here. For the case $M_k = 0$, which is the problem of signal detection, we have studied it in Section IV. Our idea of model selection is based on multiple hypothesis tests and the asymptotic distribution of the maximum of 2-dimensional (2-D) Gaussian random fields.

Theorem 1: Let $\eta(\boldsymbol{\chi})$ be a zero mean and unit variance Gaussian random field defined for $\boldsymbol{\chi} = [r_1, \; r_2]^T$ inside a 2-D rectangular domain $\mathbb{T}$. Let $\rho(\boldsymbol{\chi}, \boldsymbol{\chi}') = E\{\eta(\boldsymbol{\chi})\eta(\boldsymbol{\chi}')\}$ be the covariance function of η. Then asymptotically in u,

$$\Pr\left[\sup_{\boldsymbol{\chi}\in\mathbb{T}} \eta(\boldsymbol{\chi}) > u \right] \approx \int_{\mathbb{T}} |\det \mathbf{\Lambda}(\boldsymbol{\chi})|^{1/2} d\boldsymbol{\chi} \frac{u e^{-u^2/2}}{(2\pi)^{3/2}}, \tag{27}$$

where $\mathbf{\Lambda}(\boldsymbol{\chi})$ is given by

$$\mathbf{\Lambda}(\boldsymbol{\chi}) = \left[\begin{array}{cc} \frac{\partial^2 \rho(\boldsymbol{\chi},\boldsymbol{\chi}')}{\partial r_1^2} & \frac{\partial^2 \rho(\boldsymbol{\chi},\boldsymbol{\chi}')}{\partial r_1 \partial r_2} \\ \frac{\partial^2 \rho(\boldsymbol{\chi},\boldsymbol{\chi}')}{\partial r_1 \partial r_2} & \frac{\partial^2 \rho(\boldsymbol{\chi},\boldsymbol{\chi}')}{\partial r_2^2} \end{array} \right]\Bigg|_{\boldsymbol{\chi}'=\boldsymbol{\chi}}. \tag{28}$$

Proof: see [31].

To make use of the above theorem, it is essential to analyze the statistical property of the residual for the WLP estimates of the order M_k from the k-th channel data:

$$\mathbf{e}_k(M_k) = \mathbf{x}_k - \hat{\mathbf{\Theta}}_k(M_k) \hat{\boldsymbol{\rho}}_k, \tag{29}$$

where $\hat{\boldsymbol{\rho}}_k = [\hat{\rho}_{k,1}, \hat{\rho}_{k,2}, \ldots, \hat{\rho}_{k,M_k}]^T$,

$$\hat{\boldsymbol{\Theta}}_k(M_k) = \left[\, \hat{\boldsymbol{\theta}}_{k,1} \quad \hat{\boldsymbol{\theta}}_{k,2} \quad \ldots \quad \hat{\boldsymbol{\theta}}_{k,M_k} \,\right], \tag{30}$$

$\hat{\boldsymbol{\theta}}_{k,m} = [\hat{z}_{k,m}, \hat{z}_{k,m}^2, \ldots, \hat{z}_{k,m}^N]^T$, and $\hat{\rho}_{k,m}$ and $\hat{z}_{k,m}$ are the WLP estimates of $\rho_{k,m}$ and $z_{k,m}$, respectively, for $m = 1, 2, \ldots, M_k$ and $k = 1, 2, \ldots, K$.

In [32], it is shown that under small error assumption, the perturbation of the WLP estimates of the frequencies and damping factors $\hat{\omega}_{k,m}$ and $\hat{\alpha}_{k,m}$, $\mathbf{d}_k = [\Delta\omega_{k,1}, \ldots, \Delta\omega_{k,M_k}, \Delta\alpha_{k,1}, \ldots, \Delta\alpha_{k,M_k}]^T$, is:

$$\mathbf{d}_k \approx \mathbf{H}_k^{-1} \mathfrak{Re}\left(\mathbf{G}_k^H \mathbf{v}_k\right), \tag{31}$$

where $\Delta\omega_{k,m} = \hat{\omega}_{k,m} - \omega_{k,m}$, $\Delta\alpha_{k,m} = \hat{\alpha}_{k,m} - \alpha_{k,m}$, $\mathbf{v}_k = [v_k(1), v_k(2), \ldots, v_k(N)]^T$, and $\mathbf{G}_k$ and $\mathbf{H}_k$ are defined as:

$$\boldsymbol{\Theta}_k = \left[\, \boldsymbol{\theta}_{k,1} \quad \boldsymbol{\theta}_{k,2} \quad \ldots \quad \boldsymbol{\theta}_{k,M_k} \,\right], \tag{32}$$

$$\mathbf{P}_k = \boldsymbol{\Theta}_k \left(\boldsymbol{\Theta}_k^H \boldsymbol{\Theta}_k\right)^{-1} \boldsymbol{\Theta}_k^H, \tag{33}$$

$$\mathbf{P}_k^{\perp} = \mathbf{I}_N - \mathbf{P}_k, \tag{34}$$

$$\mathbf{D}_k = \left[\frac{\partial \boldsymbol{\theta}_{k,1}}{\partial \tilde{\omega}_{k,1}} \cdots \frac{\partial \boldsymbol{\theta}_{k,M_k}}{\partial \tilde{\omega}_{k,M_k}} \quad \frac{\partial \boldsymbol{\theta}_{k,1}}{\partial \tilde{\alpha}_{k,1}} \quad \cdots \quad \frac{\partial \boldsymbol{\theta}_{k,M_k}}{\partial \tilde{\alpha}_{k,M_k}} \right] \Bigg|_{\tilde{\omega}_{k,m}=\omega_{k,m},\ \tilde{\alpha}_{k,m}=\alpha_{k,m}}, \tag{35}$$

$$\mathbf{C}_k = \mathrm{diag}(\rho_{k,1}, \ldots, \rho_{k,M_k}, \rho_{k,1}, \ldots, \rho_{k,M_k}), \tag{36}$$

$$\mathbf{G}_k = \mathbf{P}_k^{\perp} \mathbf{D}_k \mathbf{C}_k, \tag{37}$$

$$\mathbf{H}_k = \mathfrak{Re}\left(\mathbf{G}_k^H \mathbf{G}_k\right), \tag{38}$$

with $\boldsymbol{\theta}_{k,m} = \left[z_{k,m},\ z_{k,m}^2,\ \ldots,\ z_{k,m}^N\right]^T$, $\tilde{\omega}_{k,m}$ and $\tilde{\alpha}_{k,m}$ being the variables for $\omega_{k,m}$ and $\alpha_{k,m}$, $m = 1, 2, \ldots, M_k$. According to [33], in the first-order sense, there holds the relationship between the perturbation of $\mathbf{P}_k$ and that of $\boldsymbol{\Theta}_k$ as follows:

$$\Delta\mathbf{P}_k = \boldsymbol{\Theta}_k(\boldsymbol{\Theta}_k^H\boldsymbol{\Theta}_k)^{-1}\Delta\boldsymbol{\Theta}_k^H\mathbf{P}_k^{\perp} + \mathbf{P}_k^{\perp}\Delta\boldsymbol{\Theta}_k(\boldsymbol{\Theta}_k^H\boldsymbol{\Theta}_k)^{-1}\boldsymbol{\Theta}_k^H, \tag{39}$$

and

$$\Delta\mathbf{P}_k = \hat{\boldsymbol{\Theta}}_k(\hat{\boldsymbol{\Theta}}_k^H\hat{\boldsymbol{\Theta}}_k)^{-1}\hat{\boldsymbol{\Theta}}_k^H - \boldsymbol{\Theta}_k(\boldsymbol{\Theta}_k^H\boldsymbol{\Theta}_k)^{-1}\boldsymbol{\Theta}_k^H, \tag{40}$$

$$\Delta\boldsymbol{\Theta}_k = \hat{\boldsymbol{\Theta}}_k - \boldsymbol{\Theta}_k \approx \mathbf{D}_k\left[\,\Delta\boldsymbol{\Omega}_{1k}^T \quad \Delta\boldsymbol{\Omega}_{2k}^T\,\right]^T, \tag{41}$$

where $\Delta\boldsymbol{\Omega}_{1k} = \mathrm{diag}(\Delta\boldsymbol{\omega}_{k,1}, \ldots, \Delta\omega_{k,M_k})$, $\Delta\boldsymbol{\Omega}_{2k} = \mathrm{diag}(\Delta\alpha_{k,1}, \ldots, \Delta\alpha_{k,M_k})$. Making use of (31), (39) and the small noise condition, it is derived that the fitting residual is

$$\begin{aligned}\mathbf{e}_k(M_k) &= \hat{\mathbf{P}}_k^{\perp}\mathbf{x}_k \approx \mathbf{P}_k^{\perp}\mathbf{v}_k - \Delta\mathbf{P}_k\mathbf{s}_k \\ &\approx \big[\mathbf{P}_k^{\perp} - \mathbf{G}_k\mathbf{H}_k^{-1}\mathfrak{Re}(\mathbf{G}_k^H) \\ &\quad j\mathbf{P}_k^{\perp} + \mathbf{G}_k\mathbf{H}_k^{-1}\mathfrak{Im}(\mathbf{G}_k^H)\big]\boldsymbol{\mu}_k \triangleq \mathbf{E}_k\boldsymbol{\mu}_k,\end{aligned} \tag{42}$$

where $\boldsymbol{\mu}_k = \left[\mathfrak{Re}(\mathbf{v}_k)^T\ \mathfrak{Im}(\mathbf{v}_k)^T\right]^T$, and $\mathbf{s}_k$ is the noise-free part of $\mathbf{x}_k$.

Stacking the real and imaginary parts of $\mathbf{e}_k(M_k)$, we obtain

$$\boldsymbol{\nu}_k(M_k) = \begin{bmatrix} \mathfrak{Re}(\mathbf{e}_k(M_k)) \\ \mathfrak{Im}(\mathbf{e}_k(M_k)) \end{bmatrix} = \begin{bmatrix} \mathfrak{Re}(\mathbf{E}_k) \\ \mathfrak{Im}(\mathbf{E}_k) \end{bmatrix} \boldsymbol{\mu}_k. \tag{43}$$

Since $\mathbf{v}_k$ or $\boldsymbol{\mu}_k$ is white Gaussian, it is observed from (43) that the fitting residual vector with the WLP estimates of order M_k, $\boldsymbol{\nu}_k(M_k)$, is also Gaussian with the covariance matrix

$$\begin{aligned}\mathbf{R}_k &= E\left\{\boldsymbol{\nu}_k(M_k)\boldsymbol{\nu}_k^T(M_k)\right\} \\ &= \begin{bmatrix} \mathfrak{Re}(\mathbf{E}_k)\mathfrak{Re}(\mathbf{E}_k^T) & \mathfrak{Re}(\mathbf{E}_k)\mathfrak{Im}(\mathbf{E}_k^T) \\ \mathfrak{Im}(\mathbf{E}_k)\mathfrak{Re}(\mathbf{E}_k^T) & \mathfrak{Im}(\mathbf{E}_k)\mathfrak{Im}(\mathbf{E}_k^T) \end{bmatrix} \cdot \frac{\sigma_k^2}{2} \\ &= \frac{\sigma_k^2}{2} \cdot \mathbf{R}_{0k}.\end{aligned} \tag{44}$$

The model selection criterion comes from the observation that matching the sinusoidal poles for each channel can be viewed as a problem of multiple hypothesis tests related to the Gaussian random field and the above Gaussian residual. In detail, the Gaussian random field corresponding to our particular problem has the following specific form:

$$\eta_k(\boldsymbol{\chi}) = \frac{\langle \boldsymbol{\xi}(\boldsymbol{\chi}), \boldsymbol{\nu}_k(M_k)\rangle_{\mathbf{R}_{0k}^{\dagger}}}{\|\boldsymbol{\xi}(\boldsymbol{\chi})\|_{\mathbf{R}_{0k}^{\dagger}}}, \tag{45}$$

where $\boldsymbol{\xi}(\boldsymbol{\chi}) = [\cos(\omega+\psi)\ \ldots\ \cos(\omega N+\psi)|\ \sin(\omega+\psi)\ \ldots\ \sin(\omega N+\psi)]^T$ is the sinusoidal function, $\boldsymbol{\chi} = [\omega,\ \psi]^T$, $\langle \boldsymbol{\xi}(\boldsymbol{\chi}), \boldsymbol{\nu}_k(M_k)\rangle_{\mathbf{R}_{0k}^{\dagger}}$ is the weighted inner product defined as:

$$\langle \boldsymbol{\xi}(\boldsymbol{\chi}), \boldsymbol{\nu}_k(M_k)\rangle_{\mathbf{R}_{0k}^{\dagger}} = \boldsymbol{\xi}^T(\boldsymbol{\chi})\mathbf{R}_{0k}^{\dagger}\boldsymbol{\nu}_k(M_k), \tag{46}$$

and $\|\boldsymbol{\xi}(\boldsymbol{\chi})\|_{\mathbf{R}_{0k}^{\dagger}}$ is the weighted 2-norm of the form:

$$\|\boldsymbol{\xi}(\boldsymbol{\chi})\|_{\mathbf{R}_{0k}^{\dagger}} = \sqrt{\boldsymbol{\xi}^T(\boldsymbol{\chi})\mathbf{R}_{0k}^{\dagger}\boldsymbol{\xi}(\boldsymbol{\chi})}, \tag{47}$$

where † represents Moore-Penrose pseudo-inverse. From (45), it is seen that $\eta_k(\boldsymbol{\chi})$ is a Gaussian random field defined on $\mathbb{T} = [0, 2\pi] \times [0, 2\pi]$ with mean zero and variance:

$$\begin{aligned}\mathrm{var}\left(\eta_k(\boldsymbol{\chi})\right) &= E\left\{\eta_k^2(\boldsymbol{\chi})\right\} = E\left\{\frac{\langle \boldsymbol{\xi}(\boldsymbol{\chi}), \boldsymbol{\nu}_k(M_k)\rangle^2_{\mathbf{R}_{0k}^{\dagger}}}{\|\boldsymbol{\xi}(\boldsymbol{\chi})\|^2_{\mathbf{R}_{0k}^{\dagger}}}\right\} \\ &= \frac{\boldsymbol{\xi}^T(\boldsymbol{\chi})\mathbf{R}_{0k}^{\dagger}E\left\{\boldsymbol{\nu}_k(M_k)\boldsymbol{\nu}_k^T(M_k)\right\}\mathbf{R}_{0k}^{\dagger}\boldsymbol{\xi}(\boldsymbol{\chi})}{\boldsymbol{\xi}^T(\boldsymbol{\chi})\mathbf{R}_{0k}^{\dagger}\boldsymbol{\xi}(\boldsymbol{\chi})} \\ &= \frac{\boldsymbol{\xi}^T(\boldsymbol{\chi})\mathbf{R}_{0k}^{\dagger}\boldsymbol{\xi}(\boldsymbol{\chi})}{\boldsymbol{\xi}^T(\boldsymbol{\chi})\mathbf{R}_{0k}^{\dagger}\boldsymbol{\xi}(\boldsymbol{\chi})} \cdot \frac{\sigma_k^2}{2} = \frac{\sigma_k^2}{2}.\end{aligned} \tag{48}$$

Therefore, according to Theorem 1, the asymptotic probability distribution of the statistical quantity $G_k(M_k) = \sup_{\omega,\psi} \eta_k^2(\boldsymbol{\chi})$ with respect to x, is

$$\begin{aligned}\Pr\left[G_k(M_k) > x\right] &= \Pr\left[\sup_{\omega,\psi} \eta_k^2(\boldsymbol{\chi}) > x\right] \\ &\le 2\Pr\left[\sup_{\omega,\psi} \eta_k'(\boldsymbol{\chi}) > \frac{\sqrt{2}}{\sigma_k}\sqrt{x}\right] \\ &\approx \frac{c\sqrt{x}}{\sigma_k \cdot \pi^{3/2}} e^{-x/\sigma_k^2},\end{aligned} \tag{49}$$

where

$$\eta_k'(\boldsymbol{\chi}) = \frac{\langle \boldsymbol{\xi}(\boldsymbol{\chi}), \boldsymbol{\nu}_k(M_k)\rangle_{\mathbf{R}_{0k}^{\dagger}}}{\|\boldsymbol{\xi}(\boldsymbol{\chi})\|_{\mathbf{R}_{0k}^{\dagger}}} \cdot \left(\frac{\sigma_k}{\sqrt{2}}\right)^{-1} \tag{50}$$

is a zero mean and unit variance Gaussian random field, and

$$c = \int_{\mathbb{T}} |\det \mathbf{\Lambda}_k(\boldsymbol{\chi})|^{1/2} d\boldsymbol{\chi}, \tag{51}$$

$$\mathbf{\Lambda}_k(\boldsymbol{\chi}) = \left[\begin{array}{cc} \frac{\partial^2 \rho_k(\boldsymbol{\chi},\boldsymbol{\chi}')}{\partial \omega^2} & \frac{\partial^2 \rho_k(\boldsymbol{\chi},\boldsymbol{\chi}')}{\partial \omega \partial \psi} \\ \frac{\partial^2 \rho_k(\boldsymbol{\chi},\boldsymbol{\chi}')}{\partial \omega \partial \psi} & \frac{\partial^2 \rho_k(\boldsymbol{\chi},\boldsymbol{\chi}')}{\partial \psi^2} \end{array} \right]\Bigg|_{\boldsymbol{\chi}'=\boldsymbol{\chi}}, \tag{52}$$

$$\begin{aligned} \rho_k(\boldsymbol{\chi},\boldsymbol{\chi}') &= E\left\{\eta_k'(\boldsymbol{\chi})\eta_k'(\boldsymbol{\chi}')\right\} \\ &= \frac{\langle \boldsymbol{\xi}(\boldsymbol{\chi}), \boldsymbol{\xi}(\boldsymbol{\chi}') \rangle_{\mathbf{R}_{0k}^{\dagger}}}{\|\boldsymbol{\xi}(\boldsymbol{\chi})\|_{\mathbf{R}_{0k}^{\dagger}} \cdot \|\boldsymbol{\xi}(\boldsymbol{\chi}')\|_{\mathbf{R}_{0k}^{\dagger}}}. \end{aligned} \tag{53}$$

Now we devise the sinusoidal model selection criterion by utilizing the asymptotic distribution of (49). Let ε be the pre-assigned probability of incorrect model selection. Referring to (49), our goal is to find a threshold t_k for which

$$\Pr\left[G_k(M_k) > t_k\right] \le \frac{c\sqrt{t_k}}{\sigma_k \cdot \pi^{3/2}} e^{-t_k/\sigma_k^2} = \varepsilon. \tag{54}$$

Taking logarithm on (54), the corresponding threshold t_k is the solution to

$$\ln \frac{c}{\sigma_k \cdot \pi^{3/2}} + \frac{1}{2}\ln t_k - \frac{t_k}{\sigma_k^2} = \ln \varepsilon. \tag{55}$$

According to EVT, we look for an asymptotic solution of (55) in the following form [34]:

$$t_k = A \ln 2N \cdot \left[1 + B\frac{\ln\ln 2N}{\ln 2N} + \frac{C}{\ln 2N}\right]. \tag{56}$$

Substituting (56) into (55), neglecting the minor terms, and equating terms of the same order give $A = \sigma_k^2,\ B = 1/2,\ C = \ln(c/2 \cdot \pi^{3/2} \cdot \varepsilon \cdot N)$. To sum up,

$$\Pr\left[G_k(M_k) > t_k\right] \le \varepsilon, \tag{57}$$

where

$$t_k = \sigma_k^2 \ln 2N + \frac{1}{2}\sigma_k^2 \ln\ln 2N + \sigma_k^2 \ln \frac{c}{2\pi^{3/2}\varepsilon N}. \tag{58}$$

To compute t_k, it is necessary to study the behavior of $\mathbf{\Lambda}_k(\boldsymbol{\chi})$. In the following, we explore the analytical form of the elements of $\mathbf{\Lambda}_k(\boldsymbol{\chi})$ to facilitate the computation of c. Denote $\boldsymbol{\xi}_1(\boldsymbol{\chi}) = \partial\boldsymbol{\xi}(\boldsymbol{\chi})/\partial\omega$, $\boldsymbol{\xi}_2(\boldsymbol{\chi}) = \partial\boldsymbol{\xi}(\boldsymbol{\chi})/\partial\psi$. Then at $\boldsymbol{\chi}' = \boldsymbol{\chi}$, it is derived that

$$\frac{\partial^2 \rho_k(\boldsymbol{\chi},\boldsymbol{\chi}')}{\partial \omega^2}\Bigg|_{\boldsymbol{\chi}'=\boldsymbol{\chi}} = -\frac{\|\boldsymbol{\xi}_1(\boldsymbol{\chi})\|^2_{\mathbf{R}_{0k}^{\dagger}}}{\|\boldsymbol{\xi}(\boldsymbol{\chi})\|^2_{\mathbf{R}_{0k}^{\dagger}}} + \frac{\langle \boldsymbol{\xi}_1(\boldsymbol{\chi}), \boldsymbol{\xi}(\boldsymbol{\chi})\rangle^2_{\mathbf{R}_{0k}^{\dagger}}}{\|\boldsymbol{\xi}(\boldsymbol{\chi})\|^4_{\mathbf{R}_{0k}^{\dagger}}}, \tag{59}$$

$$\frac{\partial^2 \rho_k(\boldsymbol{\chi},\boldsymbol{\chi}')}{\partial \psi^2}\Bigg|_{\boldsymbol{\chi}'=\boldsymbol{\chi}} = -\frac{\|\boldsymbol{\xi}_2(\boldsymbol{\chi})\|^2_{\mathbf{R}_{0k}^{\dagger}}}{\|\boldsymbol{\xi}(\boldsymbol{\chi})\|^2_{\mathbf{R}_{0k}^{\dagger}}} + \frac{\langle \boldsymbol{\xi}_2(\boldsymbol{\chi}), \boldsymbol{\xi}(\boldsymbol{\chi})\rangle^2_{\mathbf{R}_{0k}^{\dagger}}}{\|\boldsymbol{\xi}(\boldsymbol{\chi})\|^4_{\mathbf{R}_{0k}^{\dagger}}}, \tag{60}$$

$$\begin{aligned} \frac{\partial^2 \rho_k(\boldsymbol{\chi},\boldsymbol{\chi}')}{\partial \omega\, \partial \psi}\Bigg|_{\boldsymbol{\chi}'=\boldsymbol{\chi}} &= -\frac{\langle \boldsymbol{\xi}_1(\boldsymbol{\chi}), \boldsymbol{\xi}_2(\boldsymbol{\chi})\rangle_{\mathbf{R}_{0k}^{\dagger}}}{\|\boldsymbol{\xi}(\boldsymbol{\chi})\|^2_{\mathbf{R}_{0k}^{\dagger}}} \\ &\quad + \frac{\langle \boldsymbol{\xi}_1(\boldsymbol{\chi}), \boldsymbol{\xi}(\boldsymbol{\chi})\rangle_{\mathbf{R}_{0k}^{\dagger}} \cdot \langle \boldsymbol{\xi}_2(\boldsymbol{\chi}), \boldsymbol{\xi}(\boldsymbol{\chi})\rangle_{\mathbf{R}_{0k}^{\dagger}}}{\|\boldsymbol{\xi}(\boldsymbol{\chi})\|^4_{\mathbf{R}_{0k}^{\dagger}}}. \end{aligned} \tag{61}$$

With the analytical form of the elements of $\mathbf{\Lambda}_k(\boldsymbol{\chi})$ in (59)–(61), the quantity c of (51), that is the integral of $|\det\mathbf{\Lambda}_k(\boldsymbol{\chi})|^{1/2}$ over the domain $\mathbb{T} = [0, 2\pi] \times [0, 2\pi]$, can be calculated in a numerical way [35].

The next question is to calculate $G_k(M_k)$, that is, to find $\hat{\omega}$, $\hat{\psi}$, such that:

$$\begin{aligned} [\hat{\omega},\ \hat{\psi}] &= \arg\max_{\omega,\psi} \eta_k^2(\boldsymbol{\chi}) \\ &= \arg\max_{\omega,\psi} \frac{\left(\boldsymbol{\nu}_k(M_k)^T \mathbf{R}_{0k}^{\dagger} \boldsymbol{\xi}(\boldsymbol{\chi})\right)^2}{\boldsymbol{\xi}(\boldsymbol{\chi})^T \mathbf{R}_{0k}^{\dagger} \boldsymbol{\xi}(\boldsymbol{\chi})}. \end{aligned} \tag{62}$$

Defining $\hat{q} = (\boldsymbol{\nu}_k(M_k)^T \mathbf{R}_{0k}^{\dagger} \boldsymbol{\xi}(\hat{\boldsymbol{\chi}}))/(\boldsymbol{\xi}(\hat{\boldsymbol{\chi}})^T \mathbf{R}_{0k}^{\dagger} \boldsymbol{\xi}(\hat{\boldsymbol{\chi}}))$, $\hat{\boldsymbol{\chi}} = [\hat{\omega},\ \hat{\psi}]^T$, we have:

$$2\hat{q}\boldsymbol{\xi}(\hat{\boldsymbol{\chi}})^T \mathbf{R}_{0k}^{\dagger} \boldsymbol{\xi}(\hat{\boldsymbol{\chi}}) - 2\boldsymbol{\nu}_k(M_k)^T \mathbf{R}_{0k}^{\dagger} \boldsymbol{\xi}(\hat{\boldsymbol{\chi}}) = 0. \tag{63}$$

Integrating both sides of (63) with respect to the variable q for $\hat{q}$, we know that $\hat{q}$ is the optimum value of q such that

$$\hat{q} = \arg\min_{q} \left(q^2 \boldsymbol{\xi}(\hat{\boldsymbol{\chi}})^T \mathbf{R}_{0k}^{\dagger} \boldsymbol{\xi}(\hat{\boldsymbol{\chi}}) - 2q\boldsymbol{\nu}_k(M_k)^T \mathbf{R}_{0k}^{\dagger} \boldsymbol{\xi}(\hat{\boldsymbol{\chi}}) \right). \tag{64}$$

Substituting $\hat{q} = (\boldsymbol{\nu}_k(M_k)^T \mathbf{R}_{0k}^{\dagger} \boldsymbol{\xi}(\hat{\boldsymbol{\chi}}))/(\boldsymbol{\xi}(\hat{\boldsymbol{\chi}})^T \mathbf{R}_{0k}^{\dagger} \boldsymbol{\xi}(\hat{\boldsymbol{\chi}}))$ into (64), we see that $\hat{q}$ and $\hat{\boldsymbol{\chi}}$ minimize $-\eta_k^2(\boldsymbol{\chi})$, and thus using these values, $G_k(M_k)$ will be obtained. Now we reformulate (64) as:

$$\begin{aligned} \hat{q} &= \arg\min_{q} \Big(q^2 \boldsymbol{\xi}(\hat{\boldsymbol{\chi}})^T \mathbf{R}_{0k}^{\dagger} \boldsymbol{\xi}(\hat{\boldsymbol{\chi}}) \\ &\qquad - 2q\boldsymbol{\nu}_k(M_k)^T \mathbf{R}_{0k}^{\dagger} \boldsymbol{\xi}(\hat{\boldsymbol{\chi}}) \Big) \\ &= \arg\min_{q} \big(\boldsymbol{\nu}_k(M_k) - q\boldsymbol{\xi}(\hat{\boldsymbol{\chi}})\big)^T \mathbf{R}_{0k}^{\dagger} \big(\boldsymbol{\nu}_k(M_k) \\ &\qquad - q\boldsymbol{\xi}(\hat{\boldsymbol{\chi}})\big). \end{aligned} \tag{65}$$

Consequently, $\hat{\boldsymbol{\chi}}$ is obtained by solving the following LS problem

$$\begin{aligned} [\hat{q},\ \hat{\omega},\ \hat{\psi}] = \arg\min_{q,\omega,\psi} &\big(\boldsymbol{\nu}_k(M_k) - q\boldsymbol{\xi}(\boldsymbol{\chi})\big)^T \\ &\times \mathbf{R}_{0k}^{\dagger} \big(\boldsymbol{\nu}_k(M_k) - q\boldsymbol{\xi}(\boldsymbol{\chi})\big), \end{aligned} \tag{66}$$

where the parameters $\hat{q}$ and $\hat{\psi}$ are converted into the functions of $\hat{\omega}$[1]. As a result, the nonlinear parameter $\hat{\omega}$ is found with one-dimensional search, $\hat{\psi}$ is calculated from $\hat{\omega}$, and then $G_k(M_k)$ is computed. Here, the search is conducted with the trust-region-reflective algorithm bearing the local convergence property with quadratic rate of convergence [36], and the initial value from the minimum grid point.

In practice, the true values of the parameters contained in the weighting matrices $\mathbf{R}_{0k}^{\dagger}$ and the noise levels σ_k^2 $(k = 1, 2, \ldots, K)$ are unknown. However, when the signal-to-noise ratio (SNR) is higher than the threshold value (or σ_k^2 is small enough), the parameter estimates $\hat{\alpha}_m$ and $\hat{\omega}_m$ of (26), $m = 1, 2, \ldots, M$, will be close to their true values, with which we can estimate $\mathbf{R}_{0k}^{\dagger}$ and σ_k^2 $(k = 1, 2, \ldots, K)$ accurately. Therefore, in the algorithm implementation, it is reasonable to construct the stochastic field $\eta_k'(\boldsymbol{\chi})$ of (50), and to determine $G_k(M_k)$ and the threshold value t_k in the same way

as (66) and (58), but with the estimated $\mathbf{R}_{0k}$ and σ_k^2. In addition, from the derivation of (29) –(44), the covariance matrix keeps the same expression of (44) if the parameter estimates $\hat{z}_{k,m}$ are closer to their true values. Therefore, in practice, the sinusoidal parameter estimates from the multi-channel data and the MC-WLP estimator, $\hat{\alpha}_m,\ \hat{\omega}_m$, are utilized in the construction of the stochastic field $\eta_k'(\boldsymbol{\chi})$ of (50), which are more accurate than that from the single-channel data.

According to (45), for the k-th channel ($k = 1, 2, \ldots, K$), the quantity $G_k(m) = \sup_{\omega,\psi} \eta_k^2(\boldsymbol{\chi})$ can be viewed as the maximum "weighted" correlation between the fitting residual $\mathbf{e}_k(m)$ (or $\boldsymbol{\nu}_k(m)$) of order m and the sinusoidal function $\boldsymbol{\xi}(\boldsymbol{\chi})$ scaled by the "weighted" energy of $\boldsymbol{\xi}(\boldsymbol{\chi})$. In the above analysis, we show that, when fitting the signal $\mathbf{x}_k$ with the accurate sinusoidal pole estimates of the correct model order M_k, the noiseless part of $\mathbf{x}_k$, $\mathbf{s}_k$, will be canceled out by the estimated vectors $\hat{\boldsymbol{\theta}}_{k,m},\ m = 1, 2, \ldots, M_k$, as much as possible, and the residual $\mathbf{e}_k(M_k)$ is just Gaussian noise and uncorrelated with any sinusoidal function. Therefore, it is reasonable to regard $G_k(M_k)$ as small with high probability. On the other hand, if we fit the signal $\mathbf{x}_k$ with $M_k' < M_k$ sinusoidal poles, there will be at least one sinusoidal pole not canceled out, and the remained part $\mathbf{e}_k(M_k')$ contains noticeable sinusoids. Ignoring the difference in $\mathbf{R}_{0k}^{\dagger}$ for different order m, it is observed that $G_k(M_k')$ is obviously larger. As a result, the sinusoidal model selection criterion with the MC-WLP estimates $\hat{z}_1,\ \hat{z}_2,\ \ldots,\ \hat{z}_M$, for the k-th channel, is proposed as follows:

- Step 1. Estimate the amplitudes of $\mathbf{x}_k$ corresponding to the sinusoidal poles $\hat{z}_1,\ \hat{z}_2,\ \ldots,\ \hat{z}_M$:
$$[\,\hat{\lambda}_{k,1} \quad \hat{\lambda}_{k,2} \quad \ldots \quad \hat{\lambda}_{k,M}\,]^T = (\hat{\boldsymbol{\Theta}}^H\hat{\boldsymbol{\Theta}})^{-1}\hat{\boldsymbol{\Theta}}^H\mathbf{x}_k.$$
- Step 2. Sort $\hat{\lambda}_{k,1},\ \hat{\lambda}_{k,2},\ \ldots,\ \hat{\lambda}_{k,M}$ as $\hat{\lambda}'_{k,1},\ \hat{\lambda}'_{k,2},\ \ldots,\ \hat{\lambda}'_{k,M}$ in terms of their moduli.
- Step 3. Set $i_0 = 1$.
- Step 4. Fit the signal $\mathbf{x}_k$ with the selected sinusoidal poles corresponding to $\hat{\lambda}'_{k,i},\ i = 1, 2, \ldots, i_0$.
- Step 5. Estimate $\mathbf{R}_{0k}$ by (44), and σ_k^2 by
$$\hat{\sigma}_k'^2 = \mathbf{x}_k^H(\mathbf{I}_N - \hat{\boldsymbol{\Theta}}_k'(\hat{\boldsymbol{\Theta}}_k'^H\hat{\boldsymbol{\Theta}}_k')^{-1}\hat{\boldsymbol{\Theta}}_k'^H)\mathbf{x}_k/N,$$
for $k = 1, 2, \ldots, K$, where
$$\hat{\boldsymbol{\Theta}}_k' = [\,\hat{\boldsymbol{\theta}}'_{k,1} \quad \hat{\boldsymbol{\theta}}'_{k,2} \quad \ldots \quad \hat{\boldsymbol{\theta}}'_{k,i_0}\,],$$
$$\hat{\boldsymbol{\theta}}'_{k,i} = [\hat{z}_{k,i},\ \hat{z}_{k,i}^2,\ \ldots,\ \hat{z}_{k,i}^N]^T,$$
and with the sinusoidal parameters corresponding to $\hat{\lambda}'_{k,i},\ i = 1, 2, \ldots, i_0$.
- Step 6. Construct the statistical quantity $G_k(i_0)$, compute the threshold $t_k(i_0)$, and perform the hypothesis test. If $G_k(i_0) \le t_k(i_0)$, then the model selection is finished, and the selected sinusoidal poles belong to the k-th channel. Otherwise, go to Step 7.
- Step 7. Set $i_0 = i_0 + 1$, and go to Step 4.

The above sinusoidal model selection method is termed as the EVT selector. Note that the testing statistical quantity $G_k(i_0)$ is the maximum weighted correlation between $\boldsymbol{\nu}_k(i_0)$ and $\boldsymbol{\xi}(\boldsymbol{\chi})$ scaled by the weighted energy of $\boldsymbol{\xi}(\boldsymbol{\chi})$, and the EVT selector is also able to be applied in the single-channel setup.

IV. Performance Analysis

A. Consistency of Detection of Distinct Poles

Regarding the consistency of the proposed MC-MOE, it is straightforward that on the asymptotic SNR condition: $\mathrm{SNR} \to \infty$, $\mathbf{X} \to \mathbf{S}$, and then $\hat{\mathbf{U}}_s^{tb}$ converges to the version from $\mathbf{S}$. Furthermore, for the matrix $\hat{\mathbf{U}}_s^{tb} \in \mathbb{C}^{(L-1)\times 2M}$, its M last singular values $\hat{\gamma}_i \to 0,\ i = M+1, M+2, \ldots, 2M$, and then $E(M) \to 0$. On the other hand, according to the analysis in the SAMOS method [28], $E(\tilde{M})$ will normally not be equal to zero for other $\tilde{M}$ values. As a result, when $\mathrm{SNR} \to \infty$, M will be the minimal of $E(\tilde{M})$ with probability one, which completes the proof of the asymptotic consistency of the MC-MOE with respect to SNR.

In practice, the probability of correct detection cannot be guaranteed to be one, and there is also threshold behavior at certain SNR, above which it is close to one and below which it is rapidly decreased to near zero. This threshold behavior is largely attributed to the occurrence of "subspace swapping" [37].

B. Computational Complexity of Parameter Estimation

In the MC-WLP parameter estimation for the sinusoids from the multiple channels, the main computational complexity (taking only the multiplications into account) in one iteration consists of three main parts from (24): (i) K times of matrix multiplication of $\mathbf{X}_k^H\mathbf{W}_0\mathbf{X}_k$ and $\mathbf{X}_k^H\mathbf{W}_0\mathbf{b}_k$; (ii) matrix inversion of $\sum_{k=1}^K \sigma_k^{-2}\mathbf{X}_k^H\mathbf{W}_0\mathbf{X}_k$; (iii) construction of the weighting matrix $\mathbf{W}_0$, among which the third part occupies most of the computation, and requires FLOPs of $\mathcal{O}(N^3)$ totally. Normally $K \ll N$, and the whole computational complexity is not dominated by K, which means that the computation for the multi-channel signals is nearly the same as that for the single-channel signal. On the other hand, we can also make the multi-channel sinusoidal parameter estimation channel by channel, followed by the weighted least squares (WLS) refinement, which requires K times of the weighting matrix construction, and thus the computational complexity of $\mathcal{O}(KN^3)$ instead.

C. Parameter Estimation Accuracy

In parameter estimation, minimum variance unbiased estimator is often desired [10], which means that the estimator is unbiased and its variance is minimum. Usually, the accuracy of the devised estimator is evaluated with the mean square error (MSE): $\mathrm{MSE}(\hat{x}) = E\{(\hat{x} - x)^2\}$ with x and $\hat{x}$ being the true value and its estimate, respectively, where bias and variance are involved. When the SNR is sufficiently high, the MSE of the m-th pole $z_m,\ m = 1, 2, \ldots, M$, is [38]
$$\mathrm{MSE}(\hat{z}_m) = \frac{1}{|\beta|^2}\boldsymbol{\mu}_m^H\mathbf{C}_{\hat{\mathbf{a}}}\boldsymbol{\mu}_m, \tag{67}$$
where $\mathbf{C}_{\hat{\mathbf{a}}}$ is the covariance matrix of $\hat{\mathbf{a}}$:
$$\mathbf{C}_{\hat{\mathbf{a}}} = E\left\{(\hat{\mathbf{a}} - \mathbf{a})(\hat{\mathbf{a}} - \mathbf{a})^H\right\} = \left(\sum_{k=1}^K \sigma_k^{-2}\mathbf{S}_k^H \cdot (\mathbf{A}_0\mathbf{A}_0^H)^{-1} \cdot \mathbf{S}_k\right)^{-1}, \tag{68}$$
$$\boldsymbol{\mu}_m = [\,z_m^{M-1} \quad \ldots \quad z_m \quad 1\,]^H, \tag{69}$$
$$\beta = Mz_m^{M-1} + \sum_{j=1}^{M-1}(M-j)z_m^{M-j-1}a_j, \tag{70}$$

and the MSEs of the frequency ω_m and damping factor α_m estimates are expressed as [39]:

$$\mathrm{MSE}(\hat{\omega}_m) = \mathrm{MSE}(\hat{\alpha}_m) = \frac{1}{2e^{-2\alpha_m}}\mathrm{MSE}(\hat{z}_m). \tag{71}$$

It is difficult to prove that for multi-channel multiple-tone signal, the MSE of the MC-WLP estimator, (71), is equivalent to CRLB theoretically. However, when the data length or SNR is large enough, the WLP-based estimate will converge to its globally optimum solution [29]. This is also supported by simulation results in Section V. In addition, following the methodology in [40], it can be proved that the MC-WLP estimator for the multi-channel undamped single-tone signals is unbiased with variance:

$$\mathrm{var}(\hat{\omega}_1) = \mathrm{var}(\hat{\alpha}_1) = \frac{1}{2}\mathrm{var}(\hat{z}_1) \approx \frac{6}{N^3 \sum_{k=1}^{K} \mathrm{SNR}_k}, \tag{72}$$

for large data length N with SNR_k being the SNR of the k-th channel, which is equal to the asymptotic CRLB [41]. In such a case, the MC-WLP method is proved as a minimum variance unbiased estimator.

D. Existence Hypothesis Test and its Threshold Performance

It is assumed that there exists the sinusoidal signal in all the multiple channels in Section III-C. Nevertheless, in practice, it is also possible that there is noise only in some channels. So, it is necessary to check the existence of signals for each channel prior to sinusoidal model selection. This is a binary hypothesis test problem for the k-th ($k = 1, 2, \ldots, K$) channel:

$$\begin{aligned} &\mathcal{H}_{k0} : \text{there is noise only;} \\ &\mathcal{H}_{k1} : \text{there exists signal.} \end{aligned} \tag{73}$$

In detail, suppose that for the k-th channel:

$$x_k(n) = v_k(n), \tag{74}$$

for $n = 1, 2, \ldots, N$, and $k = 1, 2, \ldots, K$, and fit $\mathbf{x}_k$ with the sinusoidal function $\boldsymbol{\xi}$ in an LS way similar to Section III:

$$\begin{aligned} G_{0k} &= \sup_{q,\omega,\psi} \boldsymbol{\nu}_{0k}^T \boldsymbol{\nu}_{0k} - \left(\boldsymbol{\nu}_{0k} - q\boldsymbol{\xi}\right)^T \left(\boldsymbol{\nu}_{0k} - q\boldsymbol{\xi}\right) \\ &= \frac{1}{N}\left\{\sum_{n=1}^{N} \mathfrak{Re}(x_k(n)) \cos\tau(n) \right. \\ &\qquad \left. + \sum_{n=1}^{N} \mathfrak{Im}(x_k(n)) \sin\tau(n)\right\}^2, \end{aligned} \tag{75}$$

where $\boldsymbol{\nu}_{0k} = [\,\mathfrak{Re}(\mathbf{x}_k^T) \quad \mathfrak{Im}(\mathbf{x}_k^T)\,]^T$, $\tau(n) = \hat{\omega}n + \hat{\psi}$. Based on the ideas in Section III, the hypothesis $\mathcal{H}_{k0}$ is accepted if $G_{0k} \le t_{0k}$, or rejected otherwise, where t_{0k} is the threshold defined as $\Pr[G_{0k} > t_{0k}] = \varepsilon$. According to Theorem 1 and following the similar steps in Section III, the asymptotic distribution of G_{0k} is derived as:

$$\Pr[G_{0k} > x] \le \frac{c_0\sqrt{x}}{\sigma_k \cdot \pi^{3/2}} e^{-x/\sigma_k^2}, \tag{76}$$

and the corresponding threshold value t_{0k} is:

$$t_{0k} = \sigma_k^2 \ln 2N + \frac{1}{2}\sigma_k^2 \ln\ln 2N + \sigma_k^2 \ln\frac{c_0}{2\pi^{3/2}\varepsilon N}, \tag{77}$$

where

$$\rho_{0k}(\boldsymbol{\chi}, \boldsymbol{\chi}') = \frac{\langle \boldsymbol{\xi}(\boldsymbol{\chi}), \boldsymbol{\xi}(\boldsymbol{\chi}')\rangle}{\|\boldsymbol{\xi}(\boldsymbol{\chi})\| \cdot \|\boldsymbol{\xi}(\boldsymbol{\chi}')\|}, \tag{78}$$

$$\boldsymbol{\Lambda}_{0k}(\boldsymbol{\chi}) = \left[\begin{array}{cc} \frac{\partial^2 \rho_{0k}(\boldsymbol{\chi},\boldsymbol{\chi}')}{\partial\omega^2} & \frac{\partial^2 \rho_{0k}(\boldsymbol{\chi},\boldsymbol{\chi}')}{\partial\omega\partial\psi} \\ \frac{\partial^2 \rho_{0k}(\boldsymbol{\chi},\boldsymbol{\chi}')}{\partial\omega\partial\psi} & \frac{\partial^2 \rho_{0k}(\boldsymbol{\chi},\boldsymbol{\chi}')}{\partial\psi^2} \end{array}\right]\Bigg|_{\boldsymbol{\chi}'=\boldsymbol{\chi}}, \tag{79}$$

$$c_0 = \int_{\mathbb{T}} |\det\boldsymbol{\Lambda}_{0k}(\boldsymbol{\chi})|^{1/2} d\boldsymbol{\chi} \approx \frac{2}{\sqrt{3}} N\pi^2. \tag{80}$$

Next, we analyze the threshold signal strength required for detecting the presence of a single undamped sinusoid:

$$\begin{aligned} x_k(n) &= A_{k,1} e^{j(\omega_{k,1}n + \psi_{k,1})} \\ &= A_{k,1}\cos\zeta(n) + jA_{k,1}\sin\zeta(n), \end{aligned} \tag{81}$$

for $k = 1, 2, \ldots, K$, where $\zeta(n) = \omega_{k,1}n + \psi_{k,1}$, and $A_{k,1}, \psi_{k,1}$ and $\omega_{k,1}$ represent the real-valued amplitude, initial phase and frequency, respectively. To focus on the problem of detection threshold analysis, here we assume that $\psi_{k,1}, \omega_{k,1}$ and σ_k^2 are known *a priori*. Then we have that:

$$\begin{aligned} G_{0k} &= \sup_q \boldsymbol{\nu}_{0k}^T \boldsymbol{\nu}_{0k} - \left(\boldsymbol{\nu}_{0k} - q\boldsymbol{\xi}_0\right)^T \left(\boldsymbol{\nu}_{0k} - q\boldsymbol{\xi}_0\right) \\ &= \boldsymbol{\nu}_{0k}^T \boldsymbol{\nu}_{0k} - \left(\boldsymbol{\nu}_{0k} - \hat{q}\boldsymbol{\xi}_0\right)^T \left(\boldsymbol{\nu}_{0k} - \hat{q}\boldsymbol{\xi}_0\right), \end{aligned} \tag{82}$$

where $\boldsymbol{\xi}_0 = [\cos(\omega_{k,1} + \psi_{k,1}) \ \ldots \ \cos(\omega_{k,1}N + \psi_{k,1})|\ \sin(\omega_{k,1} + \psi_{k,1}) \ \cdots \ \sin(\omega_{k,1}N + \psi_{k,1})]^T$, and

$$\begin{aligned} \hat{q} &= \arg\min_q \left(\boldsymbol{\nu}_{0k} - q\boldsymbol{\xi}_0\right)^T \left(\boldsymbol{\nu}_{0k} - q\boldsymbol{\xi}_0\right) \\ &= A_{k,1} + \frac{1}{N}\boldsymbol{\mu}_k^T \boldsymbol{\xi}_0. \end{aligned} \tag{83}$$

As a result, when the SNR is sufficiently large compared with the data length N, we obtain

$$G_{0k} \approx N A_{k,1}^2. \tag{84}$$

Hence, the sinusoidal power required for detection is:

$$A_{k,1}^2 > \frac{1}{N}\left[\sigma_k^2 \ln 2N + \frac{1}{2}\sigma_k^2 \ln\ln 2N + \sigma_k^2 \ln\frac{c_0}{2\pi^{3/2}\varepsilon N}\right], \tag{85}$$

and the corresponding threshold SNR of the k-th channel is

$$\mathrm{SNR}_{\mathrm{th},k} = \frac{1}{N}\left[\ln 2N + \frac{1}{2}\ln\ln 2N + \ln\frac{c_0}{2\pi^{3/2}\varepsilon N}\right]. \tag{86}$$

From (86), it is seen that with the increase of the data length N, the threshold SNR needed for existence will improve. When the data length $N \to \infty$, the detection threshold SNR: $\mathrm{SNR}_{\mathrm{th},k} \to 0$, which demonstrates the asymptotic consistency of the existence hypothesis test for undamped single-tone signal. However, in practice, the threshold SNR is somewhat higher than the theoretical value of (86) as the noise plays an obvious role in G_{0k} of (84).

TABLE I
NUMBER OF SINUSOIDS IN EACH CHANNEL

k	1	2	3	4	5
M_k	3	4	4	5	5

TABLE II
SINUSOIDAL POLES IN EACH CHANNEL

k	$z_{k,1}$	$z_{k,2}$	$z_{k,3}$	$z_{k,4}$	$z_{k,5}$
1	$0.95e^{j0.1\pi}$	$0.93e^{j0.3\pi}$	$0.96e^{j0.5\pi}$		
2	$0.95e^{j0.1\pi}$	$0.93e^{j0.3\pi}$	$0.96e^{j0.5\pi}$	$0.91e^{j0.9\pi}$	
3	$0.95e^{j0.1\pi}$	$0.93e^{j0.3\pi}$	$0.96e^{j0.5\pi}$	$0.92e^{j0.7\pi}$	
4	$0.95e^{j0.1\pi}$	$0.93e^{j0.3\pi}$	$0.96e^{j0.5\pi}$	$0.92e^{j0.7\pi}$	$0.94e^{j1.1\pi}$
5	$0.95e^{j0.1\pi}$	$0.93e^{j0.3\pi}$	$0.92e^{j0.7\pi}$	$0.91e^{j0.9\pi}$	$0.94e^{j1.1\pi}$

TABLE III
AMPLITUDES IN EACH CHANNEL

k	$\rho_{k,1}$	$\rho_{k,2}$	$\rho_{k,3}$	$\rho_{k,4}$	$\rho_{k,5}$
1	$2e^{j}$	$2e^{2j}$	$3e^{3j}$		
2	$2.5e^{j}$	$3e^{2j}$	$1.5e^{3j}$	$2e^{4j}$	
3	$2e^{j}$	$1.5e^{2j}$	$1.5e^{3j}$	e^{4j}	
4	$4e^{j}$	$3e^{2j}$	e^{3j}	$2e^{4j}$	$2e^{5j}$
5	$4e^{j}$	$3e^{2j}$	$2e^{3j}$	$2e^{4j}$	e^{5j}

V. SIMULATION RESULTS

Monte Carlo simulations are carried out to evaluate the performance of the proposed multi-channel sinusoidal modeling methodology, which consists of three parts: (i) detection of distinct multi-channel sinusoidal poles with the MC-MOE; (ii) frequency and damping factor estimation of multi-channel sinusoidal poles with the MC-WLP estimator; and (iii) sinusoidal model selection for each channel with the EVT selector. The performance of the detection of distinct sinusoidal poles is evaluated in terms of the probability of correct detection (PCD): $\mathrm{PCD} = S_0/S$ with S_0 and S being the number of correct detection trials and the total number of trials, respectively. The parameter estimation accuracy is evaluated using the MSE. As for the model selection, the probability of construction error (PCE): $\mathrm{PCE} = S_1/S$ is adopted with S_1 being the number of failing model selection trials. All the results provided are averages of 1000 independent runs.

In the simulation, we consider two kinds of signal from $K = 5$ channels: single-tone and multiple-tone, if not mentioned additionally. The multi-channel single-tone signal is: $s_k(n) = \rho_0 e^{(-\alpha_0 + j\omega_0)n}$, $n = 1, 2, \ldots, N$, where $N = 50$, $\rho_0 = e^{j}$, $\omega_0 = 0.4\pi$, $\alpha_0 = 0$, and the noise levels of $\{v_k(n)\}$ $(k = 1, 2, \ldots, K)$ are set equal: $\sigma_1^2 = \sigma_2^2 = \sigma_3^2 = \sigma_4^2 = \sigma_5^2$. For the multi-channel multiple-tone signal, the data length is also $N = 50$, and the parameter setting is shown in Tables I, II, and III, which indicates that there exist $M = 6$ distinct sinusoidal poles in these channels: $z_1 = 0.95e^{j0.1\pi}, z_2 = 0.93e^{j0.3\pi}, z_3 = 0.96e^{j0.5\pi}$, $z_4 = 0.92e^{j0.7\pi}, z_5 = 0.91e^{j0.9\pi}, z_6 = 0.94e^{j1.1\pi}$, where z_1 and z_2 are fully-common poles shared by all K channels. For the multiple-tone signals, the noise levels are set as $\sigma_1^2 : \sigma_2^2 : \sigma_3^2 : \sigma_4^2 : \sigma_5^2 = 1 : 2 : 3 : 2 : 1$. All the above are made with respect to the SNR of the 1st channel, defined as $\mathrm{SNR}_1 = \sigma_s^2/\sigma_1^2$ with the signal power $\sigma_s^2 = \left(\sum_{k=1}^{K}\sum_{n=1}^{N}|s_k(n)|^2\right)/\left(K \cdot N\right)$.

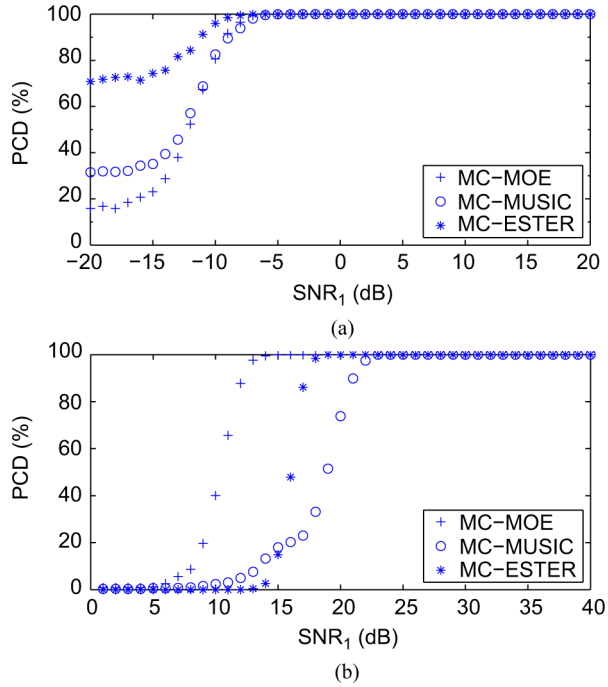

Fig. 1. PCDs of detection of distinct multi-channel sinusoidal poles versus SNR (a) single tone and (b) multiple tones.

A. Detection of Distinct Sinusoidal Poles

Before investigating the performance of the proposed MC-MOE, we construct and stack the data matrix $\overline{\mathbf{X}}_k$ $(k = 1, 2, \ldots, K)$ for each channel, and also extend the single-channel MUSIC [18] and ESTER [19] order estimators to the multi-channel scenario, which are called the multi-channel MUSIC (MC-MUSIC) and multi-channel ESTER (MC-ESTER) methods, respectively. In addition, in developing the MC-MUSIC estimator, we utilize the root MUSIC technique [1] instead of spectral MUSIC [18] to avoid the 2-D search for the frequencies and damping factors. In the evaluation, comparison is made with the MC-MUSIC and MC-ESTER methods. In [42] it is shown that the best shift-invariance characteristic of signal subspace is achieved when the data matrix is as square as possible. So here the number of rows of each data matrix $\overline{\mathbf{X}}_k$ is set as $L = \lfloor 0.5N \rfloor$ with $\lfloor u \rfloor$ denoting the largest integer less than u, which is also found empirically to result in good performance. Note that the major computational complexities of these three methods lie in the SVD of the data matrix, which is $\mathcal{O}(L^3)$.

Fig. 1 shows the PCDs of the proposed approach together with the MC-MUSIC and MC-ESTER methods for the estimation of the number of the distinct multi-channel sinusoidal poles with respect to SNR_1. It is seen that for the single-tone signals, all methods perform perfectly from $\mathrm{SNR}_1 = -5\,\mathrm{dB}$, that is with PCD of 100%. As for the multiple-tone signals, their order estimates are consistent asymptotically with respect to the SNR. In detail, the detection of the MC-MOE achieves a 100% success rate above the threshold $\mathrm{SNR}_1 = 15\,\mathrm{dB}$, while the MC-ESTER and MC-MUSIC methods are perfect when $\mathrm{SNR}_1 \geq 20\,\mathrm{dB}$ and $\mathrm{SNR}_1 \geq 23\,\mathrm{dB}$, respectively. That is, there is a threshold SNR advantage of the MC-MOE over the other two methods by more than $5\,\mathrm{dB}$.

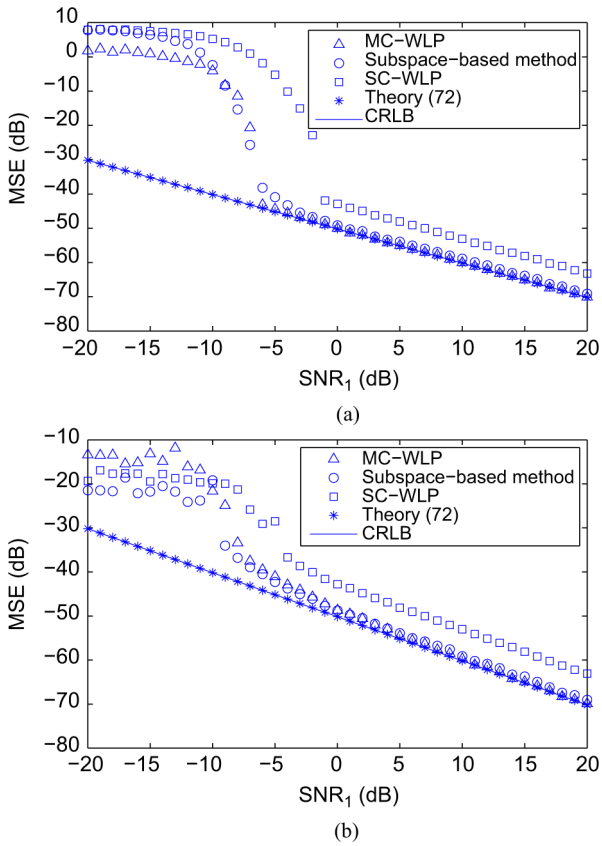

Fig. 2. MSEs for single-tone signals versus SNR (a) frequency and (b) damping factor.

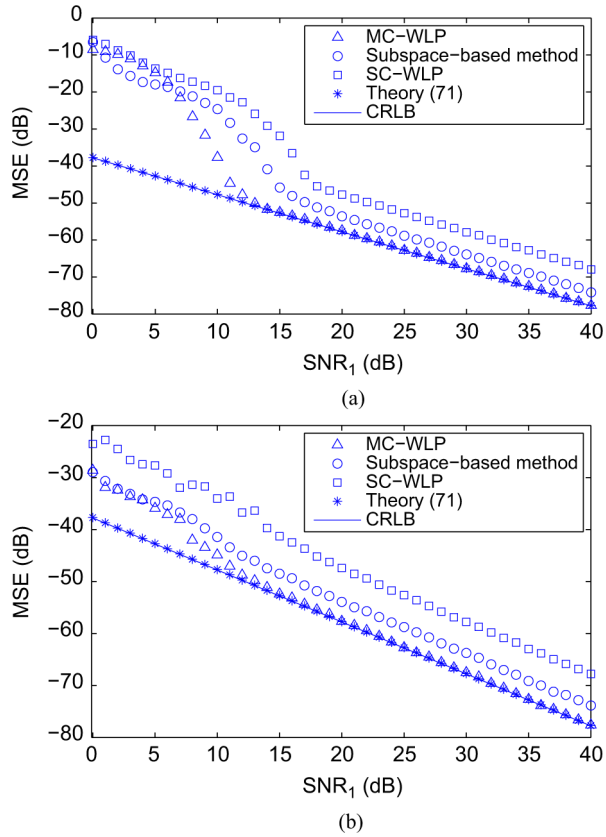

Fig. 3. MSEs for multiple-tone signals versus SNR (a) frequency and (b) damping factor.

B. Frequency and Damping Factor Estimation

Having estimated the number of the distinct multi-channel sinusoidal poles, $\hat{M}$, we then determine the frequencies and damping factors of the distinct sinusoidal poles in the multiple channels. In Section III-B, we develop the MC-WLP estimator to conduct optimum parameter estimation. In many cases, the sinusoidal parameters of the fully-common sinusoidal poles, which are shared by all the channels, are of much interest [4], [27]. Therefore, for the sake of simplicity, here we adopt the average MSEs of the parameter estimates of the fully-common poles for performance evaluation. Apart from the CRLB [27], comparison is made with the subspace-based method [2], [4] and the average of the single-channel WLP (SC-WLP) [26] method for all channels. To observe the impact of the detection of distinct multi-channel sinusoidal poles to estimation, here we use the model order estimate in the MC-MOE, $\hat{M}$, to conduct MC-WLP parameter estimation. As illustrated at the beginning, it is necessary to know the number of the cisoids in each channel and that of the fully-common sinusoidal poles prior to using the subspace-based method. So to facilitate the comparison, we assume them as known *a priori* when using the subspace-based method. We also make similar order assumption for the use of the SC-WLP method.

Figs. 2 and 3 show the frequency and damping factor estimation performance for the multi-channel single-tone and multiple-tone signals, respectively. It is observed that the threshold SNR for estimation accords with that for detection. This is because the MC-WLP estimator is a parametric method, which depends on the exact order estimate. In Fig. 2, it is seen that when the SNR is sufficiently high, the MSEs of the MC-WLP frequency and damping factor estimates are equal to their theoretical counterparts and CRLBs. Note that the MSE of the MC-WLP damping factor estimate begins to deviate from the CRLB when $\mathrm{SNR}_1 \leq 5$ dB. In fact, with the decrease of the SNR, there will occur the threshold behavior for nonlinear parameter estimation [29]. Meanwhile, the subspace-based and SC-WLP methods are not optimal, and there are about 1 dB and 7 dB gaps between their empirical MSEs and CRLB, respectively.

In Fig. 3, we find that in the perfect detection with SNR_1 range of $[15,\ 40]$ dB, the MSEs of the frequency and damping factor estimates of the MC-WLP method still attain the CRLBs, and the MC-WLP estimator is optimum. By comparison, the MSE of the SC-WLP method is about 10 dB higher, which demonstrates the estimation refinement of the multi-channel setup. In addition, the MSE of the subspace-based method has about 4 dB deviation from the CRLB. Similar phenomena have also been observed from the estimation results of the other sinusoidal poles. Moreover, it is seen from Fig. 3(a) that the MSE of the subspace-based method becomes larger, and cannot keep linear versus SNR_1 for $\mathrm{SNR}_1 \leq 18$ dB, indicating that the two-stage subspace-based method has a disadvantage in the threshold performance. Of course, the subspace-based method is more computationally efficient than the MC-WLP method because the former only needs three eigenvalue decompositions.

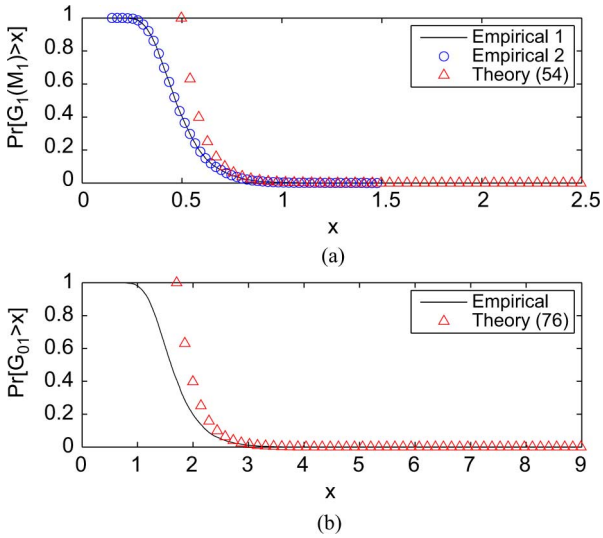

Fig. 4. Distribution of statistical quantities for hypothesis tests (a) $G_1(M_1)$ and (b) G_{01}.

C. Sinusoidal Model Selection for Each Channel

Now we have obtained the MC-WLP estimates for the parameters of the multi-channel sinusoidal poles $z_1, z_2, \ldots, z_M$. The next step is sinusoidal model selection for each channel, namely, to match the sinusoidal poles to their corresponding channels. Before model selection, it is necessary to validate the theoretical asymptotic distribution of the statistical quantity $G_k(M_k)$ and G_{0k} used in the hypothesis tests, (54) and (76), by comparing with the results from Monte Carlo simulations.

Fig. 4(a) shows the distribution results of $G_1(M_1)$ at $\mathrm{SNR}_1 = 15$ dB, where the considered multi-channel signals are parameterized with the same setting as that of the multiple-tone signals at the beginning of this section. In detail, "Empirical 1" stands for the probability distribution from the Monte Carlo simulations and using the weighting matrix $\mathbf{R}_{0k}^{\dagger}$ computed with the true parameter values; "Empirical 2" stands for the simulation result while using the estimated $\mathbf{R}_{0k}^{\dagger}$; "Theory" denotes the theoretical asymptotic distribution by (54). Note that "Empirical 1" and "Empirical 2" correspond to the ideal stochastic field $\eta_k(\boldsymbol{\chi})$ defined in (45) and the practical one we consider in the simulation of model selection, respectively. From Fig. 4(a), it is seen that the probability distribution of the maximum of the ideal stochastic field accords with that of the practical one perfectly. So it is reasonable to construct the stochastic field with the estimated weighting matrix. Moreover, when x is large and the probability of incorrect model selection, $\varepsilon = \Pr[G_1(M_1) > x]$, is small, the theoretical distributions also accord with the ones from simulations, which verifies the derived threshold value for $G_1(M_1)$, namely, t_1 of (58).

Fig. 4(b) shows the distribution results of G_{01} with $x_1(n)$ $(n = 1, 2, \ldots, N)$ being white Gaussian noise, where "Empirical" and "Theory" denote the experimental and theoretical distribution of G_{01}, respectively. It is observed that the theoretical distribution of (76) and the experimental G_{01} align well asymptotically in x, which supports the devised threshold value for G_{01}, namely, t_{01} of (77) in the sinusoidal existence hypothesis test. In addition, it is worth mentioning that the same outcomes also apply to the quantities $G_k(M_k)$ and G_{0k} for the other channels. So, it is reasonable to use the parameter estimates in the model selection as long as the SNR is high enough for optimum parameter estimation.

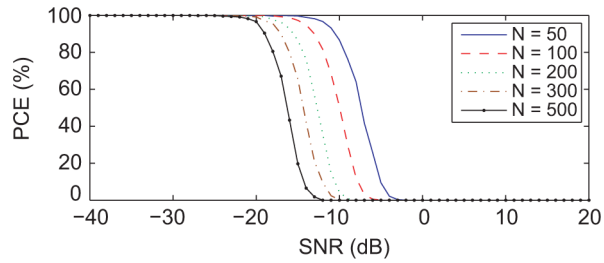

Fig. 5. Threshold performance of existence hypothesis test for undamped single tone.

Next, we show the threshold performance of the existence hypothesis test for the undamped single-tone signal: $s(n) = \rho_1 e^{j\omega_1 n}$, $n = 1, 2, \ldots, N$, with $\rho_1 = e^{j}$ and $\omega_1 = 0.4\pi$ for different data lengths $N = 50, 100, 200, 300, 500$, in Fig. 5. The probability of incorrect model selection is set as $\varepsilon = 0.02$. It is observed that the PCE is 0 at high SNR. When the SNR decreases, the PCE performance will breakdown at some SNR value, and increases rapidly to 100% afterwards. As expected, the threshold SNR will be lowered down with the increase of the data length N. Meanwhile, according to (86), the theoretical threshold SNRs are: -7.3 dB, -10.0 dB, -12.7 dB, -14.3 dB, -16.3 dB for $N = 50, 100, 200, 300, 500$, respectively. By comparison, there is about 4 dB difference between the theoretical threshold SNR and actual value, which is due to the noise in the moderate SNR zone.

Fig. 6 shows the sinusoidal model selection (including the existence hypothesis test) performance of the EVT selector for each channel with respect to SNR. Here, the probability of incorrect model selection, ε, is set as 0.02. Fig. 6(a) shows the performance for the single-tone signals, which becomes perfect at $\mathrm{SNR}_1 \geq 0$ dB for all the channels. The results for the case of multiple-tone signals are demonstrated in Fig. 6(b). It is seen that when the SNR is sufficiently high, the PCEs for the multiple channels will all become convergent around 4%, which corresponds to the preset value of ε. However, for different noise levels and tone numbers, the thresholds of the sinusoidal model selection for different channels are also different. In detail, the PCEs for the 1st, 2nd and 5th channels converge to 4% from $\mathrm{SNR}_1 = 15$ dB. By comparison, the threshold SNR_1 for the 3rd and 4th channels is higher: $\mathrm{SNR}_{1\mathrm{th}} = 20$ dB, and the EVT selector performs more poorly for the 3rd channel than the 4th one. Considering the parameter setting for the multiple-tone signals, the stronger noise and the larger tone number are disadvantageous to the performance of the proposed model selector. For comparison, we also extend the ESTER method in [19] to conduct the sinusoidal model selection by estimating the order of the signal in each channel, and show the results in Fig. 6(c). It is seen that the ESTER selector performs more poorly than the EVT selector. The former has the higher threshold SNR. In addition, note that the ESTER selector can be utilized to perform model selection when the signal is present, meanwhile the EVT

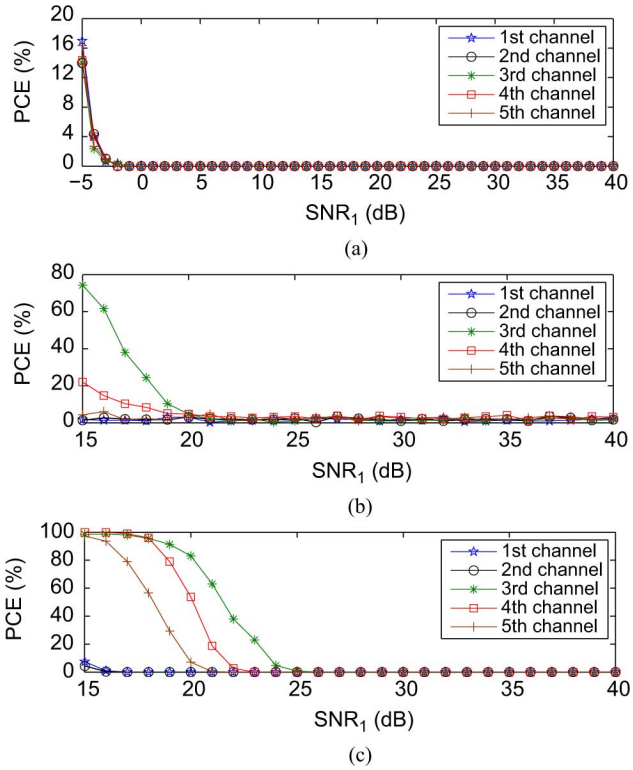

Fig. 6. PCEs of sinusoidal model selection versus SNR (a) single tone, (b) multiple tones (EVT selector), (c) multiple tones (ESTER selector).

selector can be used to perform the existence detection of sinusoidal signal.

VI. Conclusion

In this paper, we have proposed to perform the model selection and parameter estimation together for modeling damped sinusoids from multiple channels, and have devised the MC-MOE, MC-WLP estimator and EVT selector for the detection of distinct multi-channel sinusoidal poles, frequency and damping factor estimation of the multi-channel sinusoids and sinusoidal model selection for each channel, respectively. The performance of the proposed methods has been analyzed, and simulations are conducted to validate that the MC-MOE performs with lower threshold SNR than the multi-channel versions of other common detection methods. The MC-WLP estimator is statistically efficient and attains the optimum MSE performance when the SNR is sufficiently large. The EVT selector is consistent asymptotically in data length for the detection of the undamped single-tone signal, and the sinusoidal model selection is realized with a high probability for small noise.

In future work, we will go on with this topic, and extend the multi-channel sinusoidal modeling methodology to deal with joint DOA and multi-pitch estimation for audio and speech signals under the microphone array scenario.

References

[1] P. Stoica and R. L. Moses, *Spectral Analysis of Signals*. Upper Saddle River, NJ, USA: Pearson Prentice-Hall, 2005.

[2] J.-M. Papy, L. De Lathauwer, and S. Van Huffel, "Common pole estimation in multi-channel exponential data modeling," *Signal Process.*, vol. 86, no. 4, pp. 846–858, Apr. 2006.

[3] N. Sandgren, P. Stoica, F. J. Frigo, and Y. Selen, "Spectral analysis of multichannel MRS data," *J. Magn. Resonance*, vol. 175, no. 1, pp. 79–91, Jul. 2005.

[4] W. D. Clercq, B. Vanrumste, J.-M. Papy, W. V. Paesschen, and S. Van Huffel, "Modeling common dynamics in multichannel signals with applications to artifact and background removal in EEG recordings," *IEEE Trans. Biomed. Eng.*, vol. 52, no. 12, pp. 2006–2015, Dec. 2005.

[5] G. Morren, P. Lemmerling, S. Van Huffel, G. Naulaers, H. Devlieger, and P. Casaer, "Detection of autoregulation in the brain of premature infants using a novel subspace-based technique," in *Proc. 23rd Annu. Int. Conf. IEEE EMBC*, Istanbul, Turkey, Oct. 2001, vol. 2, pp. 2064–2067.

[6] J. X. Zhang, M. G. Christensen, S. H. Jensen, and M. Moonen, "Joint DOA and multi-pitch estimation based on subspace techniques," *EURASIP J. Adv. Signal Process.*, vol. 2012, no. 1, pp. 1–11, Jan. 2012.

[7] J. R. Jensen, M. G. Christensen, and S. H. Jensen, "Joint DOA and fundamental frequency estimation methods based on 2-D filtering," in *Proc. EUSIPCO*, Aalborg, Denmark, Aug. 2010, vol. 2010, pp. 2091–2095.

[8] J. R. Jensen, M. G. Christensen, and S. H. Jensen, "Nonlinear least squares methods for joint DOA and pitch estimation," *IEEE Trans. Audio, Speech, Language Process.*, vol. 21, no. 5, pp. 923–933, May 2013.

[9] E. Gudmundson, J. Ling, P. Stoica, J. Li, and A. Jakobsson, "Spectral estimation of damped sinusoids in the case of irregularly sampled data," in *Proc. IEEE ISSCS*, Iasi, Romania, Jul. 2009, pp. 1–4.

[10] S. M. Kay, *Fundamentals of Statistical Signal Processing : Estimation Theory*. Englewood Cliffs, NJ, USA: Prentice-Hall, 1993.

[11] M. G. Christensen, P. Stoica, A. Jakobsson, and S. H. Jensen, "Multi-pitch estimation," *Signal Process.*, vol. 88, no. 4, pp. 972–983, Apr. 2008.

[12] G. Morren, P. Lemmerling, and S. Van Huffel, "Decimative subspace-based parameter estimation techniques," *Signal Process.*, vol. 83, no. 5, pp. 1025–1033, May 2003.

[13] G. L. Wallstrom, R. E. Kass, A. Miller, J. F. Cohn, and N. A. Fox, "Automatic correction of ocular artifacts in the EEG: A comparison of regression-based and component-based methods," *Int. J. Psychophysiol.*, vol. 53, no. 2, pp. 105–119, Jul. 2004.

[14] H. Nam, T.-G. Yim, S. K. Han, J.-B. Oh, and S. K. Lee, "Independent component analysis of ictal EEG in medial temporal lobe epilepsy," *Epilepsia*, vol. 43, no. 2, pp. 160–164, Feb. 2002.

[15] S. M. Kay, *Fundamentals of Statistical Signal Processing : Detection Theory*. Englewood Cliffs, NJ, USA: Prentice-Hall, 1998.

[16] M. Wax and T. Kailath, "Detection of signals by information theoretic criteria," *IEEE Trans. Acoust., Speech, Signal Process.*, vol. ASSP-33, no. 2, pp. 387–392, Apr. 1985.

[17] P. Stoica and Y. Selen, "Model-order selection: A review of information criterion rules," *IEEE Signal Process. Mag.*, vol. 21, no. 4, pp. 36–47, Jul. 2004.

[18] M. G. Christensen, A. Jakobsson, and S. H. Jensen, "Sinusoidal order estimation using angles between subspaces," *EURASIP J. Adv. Signal Process.*, vol. 2009, no. 62, pp. 1–11, Jan. 2009.

[19] R. Badeau, B. David, and G. Richard, "A new perturbation analysis for signal enumeration in rotational invariance techniques," *IEEE Trans. Signal Process.*, vol. 54, no. 2, pp. 450–458, Feb. 2006.

[20] J.-M. Papy, L. De Lathauwer, and S. Van Huffel, "A shift invariance-based order-selection technique for exponential data modelling," *IEEE Signal Process. Lett.*, vol. 14, no. 7, pp. 473–476, Jul. 2007.

[21] D. C. Rife and R. R. Boorstyn, "Multiple tone parameter estimation from discrete-time observations," *Bell Syst. Tech. J.*, pp. 1389–1410, Nov. 1976.

[22] R. Schmidt, "Multiple emitter location and signal parameter estimation," *IEEE Trans. Antennas Propag.*, vol. TAP-34, no. 3, pp. 276–280, Mar. 1986.

[23] R. Roy and T. Kailath, "ESPRIT—Estimation of Signal Parameters via Rotational Invariance Techniques," *IEEE Trans. Acoust., Speech, Signal Process.*, vol. 37, no. 7, pp. 984–995, Jul. 1989.

[24] Y. T. Chan and R. P. Langford, "Spectral estimation via the high-order yule-walker equations," *IEEE Trans. Acoust., Speech, Signal Process.*, vol. ASSP-30, no. 5, pp. 689–698, Oct. 1982.

[25] B. Porat, *Digital Processing of Random Signals: Theory and Methods*. Englewood Cliffs, NJ, USA: Prentice-Hall, 1994.

[26] Y. Bresler and A. Macovski, "Exact maximum likelihood parameter estimation of superimposed exponential signals in noise," *IEEE Trans. Acoust., Speech, Signal Process.*, vol. ASSP-34, no. 5, pp. 1081–1089, Oct. 1986.

[27] F. K. W. Chan, H. C. So, and W. Sun, "Accurate estimation of common sinusoidal parameters in multiple channels," *Signal Process.*, vol. 93, no. 4, pp. 742–748, Apr. 2013.

[28] J.-M. Papy, L. De Lathauwer, and S. Van Huffel, "A shift invariance-based order selection technique for exponential data modelling," Tech. Rep [Online]. Available: ftp://www.esat.kuleuven.ac.be/pub/sista/papy/reports/jmp-05–107.ps.gz
[29] Y. Hua, A. B. Gershman, and Q. Cheng, *High-Resolution and Robust Signal Processing*. New York, NY, USA: Marcel Dekker, 2004.
[30] T. Soderstrom and P. Stoica, *System Identification*. Englewood Cliffs, NJ, USA: Prentice-Hall, 1989.
[31] R. J. Adler and J. E. Taylor, *Random Fields and Geometry*. New York, NY, USA: Springer, 2007.
[32] Z. Zhou, H. C. So, and M. G. Christensen, "Perturbation analysis of parameter estimates of damped sinusoids," Tech. Rep. [Online]. Available: http://www.create.aau.dk/mgc/publications/techzhenhua2012.pdf
[33] J. R. Magnus and H. Neudecker, *Matrix Differential Calculus with Applications in Statistics and Econometrics*. New York, NY, USA: Wiley, 1999, p. 153.
[34] R. J. Adler, "On excursion sets, tube formulas and maxima of random fields," *Ann. Appl. Probab.*, vol. 10, no. 1, pp. 1–74, Feb. 2000.
[35] T. Sauer, *Numerical Analysis*. Boston, MA, USA: Pearson, 2012.
[36] T. F. Coleman and Y. Li, "On the convergence of interior-reflective newton methods for nonlinear minimization subject to bounds," *Math. Program.*, vol. 67, no. 1-3, pp. 189–224, Oct. 1994.
[37] J. K. Thomas, L. L. Scharf, and D. W. Tufts, "The probability of a subspace swap in the SVD," *IEEE Trans. Signal Process.*, vol. 43, no. 3, pp. 730–736, Mar. 1995.
[38] Z. Zhou, H. C. So, and M. G. Christensen, "Accuracy analysis of the maximum likelihood estimates of the sinusoidal poles based on the iterative quadratic maximum likelihood method," Tech. Rep. [Online]. Available: http://www.create.aau.dk/mgc/publications/techzhenhua2013.pdf.
[39] Y. X. Yao and S. M. Pandit, "Variance of least squares estimators for a damped sinusoidal process," *IEEE Trans. Signal Process.*, vol. 42, no. 11, pp. 3016–3025, Nov. 1994.
[40] H. C. So and F. K. W. Chan, "A generalized weighted linear predictor frequency estimation approach for a complex sinusoid," *IEEE Trans. Signal Process.*, vol. 54, no. 4, pp. 1304–1315, Apr. 2006.
[41] D. N. Swingler, "Approximations to the Cramer-Rao lower bound for a single damped exponential signal," *Signal Process.*, vol. 75, no. 2, pp. 197–200, Jun. 1999.
[42] S. V. Huffel, H. Chen, C. Decanniere, and P. Vanhecke, "Algorithm for time-domain nmr data fitting based on total least squares," *J. Magn. Resonance*, ser. A, vol. 110, no. 2, pp. 228–237, Oct. 1994.

Zhenhua Zhou was born in Shanghai, China, in 1985. He received the bachelor's degree in electronic information engineering from the University of Shanghai for Science and Technology, in 2007, and the master's degree in electronic engineering from Shanghai Jiao Tong University, in 2010, both with the first GPA rank in the department. He is currently pursuing the Ph.D. degree at City University of Hong Kong. He has published several papers in peer-reviewed conference proceedings and journals. His research interest includes sinusoidal model selection and parameter estimation, optimization, tensor algebra and their application to speech and audio signal, radar signal processing. He is also interested in mechatronics.

From May 2012 to December 2012, he was a Visiting Researcher at Audio Analysis Lab, AD:MT, Univeristy of Aalborg, Aalborg, Denmark.

Mr. Zhou has served on the editorial board of the *Journal of Computer Graphics and Visualization* and has been a reviewer of *IET Signal Processing*.

H. C. So (S'90–M'95–SM'07) was born in Hong Kong. He received the B.Eng. degree from the City University of Hong Kong and the Ph.D. degree from The Chinese University of Hong Kong, both in electronic engineering, in 1990 and 1995, respectively.

From 1990 to 1991, he was an Electronic Engineer with the Research and Development Division, Everex Systems Engineering Ltd., Hong Kong. During 1995–1996, he worked as a Postdoctoral Fellow with The Chinese University of Hong Kong. From 1996 to 1999, he was a Research Assistant Professor with the Department of Electronic Engineering, City University of Hong Kong, where he is currently an Associate Professor. His research interests include statistical signal processing, fast and adaptive algorithms, signal detection, parameter estimation, and source localization.

Dr. So has been on the editorial boards of IEEE TRANSACTIONS ON SIGNAL PROCESSING, *Signal Processing*, *Digital Signal Processing*, and *ISRN Applied Mathematics*, as has been a member of the Signal Processing Theory and Methods Technical Committee of the IEEE Signal Processing Society.

Mads Græsbøll Christensen (S'00–M'05–SM'11) was born in Copenhagen, Denmark, in March 1977. He received the M.Sc. and Ph.D. degrees, in 2002 and 2005, respectively, from Aalborg University (AAU), Denmark.

He is currently an Associate Professor with the Department of Architecture, Design & Media Technology, AAU. At AAU, he is also Head of the Audio Analysis Lab, which conducts research in audio signal processing. He was formerly with the Department of Electronic Systems, AAU, and has been a Visiting Researcher at Philips Research Labs, ENST, UCSB, and Columbia University. He has published more than 100 papers in peer-reviewed conference proceedings and journals as well as one research monograph. His research interests include digital signal processing theory and methods with application to speech and audio, in particular parametric analysis, modeling, enhancement, separation, and coding.

Dr. Christensen has received several awards, including an ICASSP Student Paper Award, the Spar Nord Foundation's Research Prize for his Ph.D. thesis, a Danish Independent Research Council Young Researcher's Award, and the Statoil Prize as well as prestigious grants from the Danish Independent Research Council and the Villum Foundation's Young Investigator Programme. He has served as an Associate Editor for IEEE SIGNAL PROCESSING LETTERS.